

Active Power Regulation in Hybrid Power Plants (PV, Wind and Batteries)

Debashree Chatterjee, Thekla Louka
Electrical Power Systems and High Voltage Engineering, EPSH4-1034
May, 2024

Master's Thesis





AALBORG UNIVERSITY

STUDENT REPORT

AAU Energy

Aalborg University

<http://www.energy.aau.dk>

Title:

Active Power Regulation in
Hybrid Power Plants
(PV, Wind and Batteries)

Theme:

Master's Thesis

Project Period:

Spring Semester 2024

Project Group:

EPSH4-1034

Participant(s):

Debashree Chatterjee
Thekla Louka

Supervisor(s):

Sanjay Chaudhary
Rakesh Sinha

Page Numbers: 68

Date of Completion:

May 31, 2024

Abstract:

Inverter Based Resources (IBRs) are becoming the majority in the energy mix leading to grid instabilities due to variable production. Hybrid Power Plants (HPPs) with Battery Energy Storage Systems (BESS) can provide frequency support increasing grid stability and reliability by participating in the Ancillary Service (AS) market. The capability of the HPP with PV, WT and BESS, to provide active power control is studied in this project using various scenarios. Firstly, complementing the mismatch between the forecasted and actual production with various battery sizes is dealt with. Thereafter, the provision of frequency AS, through BESS, when there is frequency deviation in the power system is validated. Lastly, the economic impact of negative spot prices is examined. This research provides an overview of the scope of some of the services that can be provided with different BESS sizes and the significance of the impact of the market conditions.

Keywords: Active power regulation, HPP, Frequency AS, Power balance, BESS

The content of this report is freely available, but publication (with reference) may only be pursued due to agreement with the author.

Summary

The continued increasing integration of renewable energy sources (RES) and inverter-based resources, connected to the grid accelerated the innovative co-location methods such as hybrid power plants. These plants can include wind turbines, PVs and storage, coupled at the same point of connection to the grid. Hybrid power plants (HPPs) with storage can improve the system stability from the TSO perspective and also aid in increasing the plant owner's profits when providing their services to the grid through electricity markets and ancillary services (AS).

This master thesis focuses on the modelling and analysis of an HPP that includes WTs, PVs and battery energy storage systems (BESS). Real production data is used for the RES and various controllers are developed to provide active power regulation through BESS. This is accomplished with the use of a main HPP controller responsible for the plant operation, a dispatch controller dealing with production linked to market conditions and the BESS controller for the energy management and operation of the BESS. The controllers are flexible to operate under different scenarios that require active power regulation such as matching the actual plant production to the forecasted, providing primary and secondary reserves through frequency ancillary services, absorbing power and curtailing the RES in case of negative spot price.

In the first part, the state-of-the-art is presented with relevant literature studies on the topics of frequency stability, frequency ancillary services, HPP configurations and control architectures. Next, a detailed model description is provided for the HPP components and the controllers developed to operate the plant. Thereafter, the test scenarios are executed to analyse the plant's performance capabilities.

Some of the different battery sizes are tested in the first executed case to understand the requirements and constraints of the converter and energy ratings. After that, an implementation of the different frequency-sensitive modes is executed and a successful provision of primary and secondary reserves is elaborated based on the grid codes. Moreover, an economic analysis is done, in the next scenario, to highlight the advantages of providing aFRR while participating in the AS market, compared to the case when only curtailment is done to avoid additional losses.

Lastly, a discussion of the executed scenarios is presented with the conclusions drawn on project findings, followed by relevant future research.

Preface

This master's thesis is written by Debashree Chatterjee and Thekla Louka studying at Aalborg University. The project was written in the spring semester of 2024. Simulations on power systems are done on DlgSILENT PowerFactory, and for analysing results MATLAB has been used. The illustrations are created on *Microsoft Visio*.

Aalborg University, May 31, 2024

Gratitude

The authors would like to thank the supervisors, Sanjay Chaudhary and Rakesh Sinha for their availability, guidance and support throughout the project. They would also like to thank Morten Gaarde, Egill Thorbergsson, and Zhijie Ma from Eurowind Energy for their collaboration and constant support as well as Norlys Energy Trading for providing data.

Instructions for reading

The report is written in \LaTeX , and each chapter is marked with a certain number and is divided into sections. All the references used throughout the report are indicated by the method referred to as the Institute of Electrical and Electronics Engineers (IEEE). The bibliography is made in Mendeley and BibTeX, and the citations used throughout the sections are noted in the text as demonstrated below. The figures in this report are in *.pdf* format, enabling zoom-in, without the figure pixelation. Throughout this project, figures, tables, and equations will be presented in numerical order in accordance with the chapter they appear in.

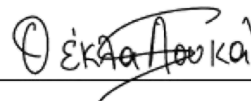
In accordance with the style, citations appear in numerical order in square brackets. If the reference appears at the end of the sentence before a period, it covers the entire sentence. When the reference appears after a period, it covers the paragraph preceding it. Examples are provided below to demonstrate this more clearly:

... [1]. Refers to the entire sentence.

... . [1] Refers to the entire paragraph.



Debashree Chatterjee



Thekla Louka

List of Abbreviations

AS	Ancillary Services
BMS	Battery Management System
BESS	Battery Energy Storage System
BRP	Balance Responsible Party
DERs	Distributed Energy Resources
DSL	DIGSILENT Simulation Language
EMS	Energy Management System
ESS	Energy Storage Systems
FCR	Frequency Containment Reserves
FCR-D	Frequency Containment Reserve for Disturbances
FCR-N	Frequency Containment Reserve for Normal Operation
FFR	Fast Frequency Response
FRR	Frequency Restoration Reserves
FSM	Frequency Sensitive Mode
GFL	Grid Following
GFM	Grid Forming
GSC	Grid Side Converter
HPP	Hybrid Power Plant
IBRs	Inverter Based Resources
KVL	Kirchoff's Voltage Law
LCoE	Levelised Cost of Energy
LFSM-O	Limited Frequency Sensitive Mode—Overfrequency

LFSM-U	Limited Frequency Sensitive Mode—Underfrequency
LPF	Low-pass filter
MPP	Maximum Power Point
MSC	Machine Side Converter
PCC	Point of Common Coupling
PLL	Phase Locked Loop
PoC	Point of Connection
PV	Photovoltaic
PWM	Pulse-width modulation
RES	Renewable Energy Sources
RoCoF	Rate of Change of Frequency
RR	Replacement Reserves
SoC	State of Charge
TSO	Transmission System Operator
UCTE	Union for the Co-ordination of Transmission of Electricity
VSC	Voltage Source Converter
WT	Wind Turbine

Contents

List of Figures	IX
List of Tables	XI
1 Introduction	1
1.1 Problem Analysis	2
1.2 Limitations	3
1.3 Methodology	3
1.4 Chapter Structures	4
2 State of the Art	6
2.1 Power System Frequency Challenges	6
2.2 Active Power Regulation	7
2.2.1 System Frequency Requirements	9
2.3 Electricity Market	9
2.4 Frequency Ancillary Services	10
2.5 HPP Configurations	11
2.6 Controller Architectures	15
2.6.1 Grid Following Mode	16
2.6.2 Current Control of VSC	17
2.6.3 PQ control loop	18
2.7 Chapter Summary	19
3 System Description and Modelling	20
3.1 System Description	20
3.2 System Modelling	21
3.2.1 Wind and PV Generation Units	21
3.2.2 Battery	21
3.2.3 External Grid	21
3.2.4 Transformers and Transmission Line	22
3.3 System Controllers	22
3.3.1 HPP Controller Architecture	22
3.3.2 Dispatch Controller	26
3.3.3 BESS Controller Architecture	26
3.3.4 Control Loop Parameters	30

3.4	Chapter Summary	31
4	Study Cases	32
4.1	Case 1: Forecast Matching	32
4.1.1	Conclusions of Case 1	35
4.2	Case 2: Frequency Ancillary Services	36
4.2.1	Conclusions of Case 2	41
4.3	Case 3: Effect of Spot Price	41
4.3.1	Conclusions of Case 3	46
4.4	Chapter Summary	46
5	Discussion	48
6	Conclusion	50
7	Future Work	51
	Bibliography	53
A	Modelling Parameters	57
A.1	Substation Transformer Parameters	57
A.2	Cable Line Parameters	57
B	Controller Block Diagrams	58
C	PowerFactory Model Diagrams	60
D	Effect of Reset in PI controller	64
E	BMS DSL code	66
F	Case 1: Forecast Matching Results	68

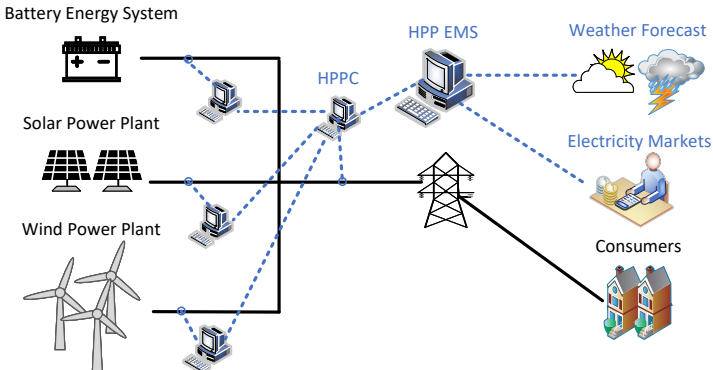
List of Figures

1.1	Power system section with a hybrid power plant [4].	1
2.1	Frequency excursion during a disturbance [12].	7
2.2	P/f droop characteristics of the control modes.	8
2.3	Time frame for ancillary services [9], [16].	11
2.4	HPP configurations, a) DC coupled PV and BESS, b) AC coupled, c) DC coupled [27].	12
2.5	Lithium iodine batteries [28].	13
2.6	PV with BESS configurations, a) without PCC, b) only AC coupled bus, c) DC coupled with a common bi-directional inverter [30].	15
2.7	Inverter based resource architecture [31].	16
2.8	Equivalent model of grid connected VSC [31].	16
2.9	Voltage and current phasors [31].	16
2.10	Simplified circuit of 3-ph grid connection of VSC [31].	17
2.11	Current control architecture of VSC [31].	18
2.12	PQ control architecture of VSC [31].	19
3.1	HPP overview.	20
3.2	HPP controller architecture.	23
3.3	FSM droop characteristics.	24
3.4	Combined P/f droop characteristics of FSM and LFSM.	25
3.5	BESS controller architecture.	27
3.6	Flowchart of BMS algorithm [17].	28
3.7	Verification of BMS model for power output and SoC.	29
3.8	Performance of BESS current controller before and after tuning.	30
3.9	SISO representation of the inner current loop for tuning.	30
4.1	RES production data and estimated forecast.	33
4.2	Power mismatch signal and battery power for 10 MW and initial SoC at 50%.	34
4.3	Power mismatch signal and battery power.	34
4.4	Frequency excursion and BESS power profile as primary response with different droop settings and convert ratings.	37
4.5	System frequency excursion and FRR response of 10 MW BESS converter.	38
4.6	System frequency excursion and FRR response of 20 MW BESS converter.	39

4.7	Frequency excursion and power of 20 MW battery, with 10 MWh, 20 MWh and 100 MWh energy ratings.	40
4.8	System frequency excursion for under-frequency and over-frequency events with a support from a 20 MW BESS providing FCR and FRR response. . .	40
4.9	Spot price profile for 14 April 2024.	42
4.10	RES production profiles based on different curtailment scenarios.	42
4.11	System frequency during different tested scenarios.	43
B.1	Enlarged figure of HPP controller architecture.	58
B.2	Enlarged figure of BESS controller architecture.	59
C.1	Schematic representation of the HPP controller DSL model developed in PowerFactory.	60
C.2	Schematic representation of the frequency control included in HPP controller. .	61
C.3	Schematic representation of the dispatch controller DSL model.	61
C.4	Schematic representation of the BESS controller.	62
C.5	Schematic representation of the P-Q control in the BESS controller.	62
C.6	Schematic representation of the current control in the BESS controller. . . .	63
D.1	Secondary response reference power signal for BESS with and without reset. .	64
D.2	Secondary response reference power signal for BESS with and without re-set for upward and downward regulation.	65
F.1	Power mismatch signal and battery power for 5 MW and 10 MW.	68
F.2	Power mismatch signal and battery power for 20 MW.	68

List of Tables

2.1	Grid code settings in DK1 for LFSM-U, LFSM-O and FSM [17], [15].	8
2.2	System frequency requirements [16], [15].	9
2.3	Ancillary services requirements [16], [8], [23].	10
3.1	BMS test reference signals.	28
3.2	Control loop parameter values.	31
4.1	Cases summary and settings in the controllers.	32
4.2	BESS performance based on sizes for average mismatch of 3.2 MW and total deficit of 7.5 %.	35
4.3	Activation time criteria for FSM and LFSM active power response for Power Park Module (PPM) for CE and Nordic area [36], [37].	36
4.4	FCR performance at FSM droop for different BESS converter ratings.	37
4.5	Frequency nadir based on LFSM droop and BESS converter ratings.	38
4.6	Secondary frequency response of the HPP based on BESS converter ratings.	39
4.7	Tests executed for system frequency support.	43
4.8	Revenue obtained by charging the 1 MW BESS.	44
4.9	Losses prevented by curtailing the WT production by 100%.	44
4.10	Losses prevented by curtailing the PV production by 100%.	45
4.11	Net revenue that is generated by charging the BESS 1 MW on the relevant cases and curtailing the RES.	45
4.12	HPP revenue though aFRR participation based on RES contribution.	46
A.1	Substation transformer parameters.	57
A.2	Cable Line 1 parameters.	57



from plant owner's perspective. [3]

With Energy Storage Systems (ESS), HPPs can provide power balance and Ancillary Services (AS) to the grid based on the grid code and service requirements. Regulating the supply from hybrid plants ensures the stability and reliability of the power systems. The plant owners can maximize their profit by controlling the active and reactive power through the Energy Management System (EMS), in conjunction with the specially designed plant controllers.[3]

Due to forecasting deviations, generation might not match the actual production causing power fluctuations. Implementing forecasting algorithms like Multistep-ahead forecasting and other predictive algorithms as cited in [5] and considering the energy market price forecasting as stated in [6], HPPs can store or provide energy to stabilize the power system. This increases the profitability of the power market but also creates opportunities for ancillary services. To achieve these functions HPP needs ESS to complement the plant's production and advanced controllers which can react and regulate power output in case of an unbalance in the grid. In HPPs, it is preferable to regulate the generation sources collectively to account for the impact that each unit's interaction with the others has on the system. [7]

1.1 Problem Analysis

This project focuses on the impact of an HPP with energy storage on the grid frequency and stability by providing active power regulation i.e. balancing the actual production and the forecasted production or through ancillary services for grid frequency support.

The main objective of this project can be divided into the following:

- Active power balance by matching the actual production and the forecasted production using a storage unit in an HPP.
- Respond to frequency fluctuations in the grid and provide ancillary frequency support services.
- Analyse the economic implications of the negative spot price.

The main tasks are identified as follows:

- Design of the HPP and its components.
- Develop controllers for each unit (eg. BESS) managing their supply and the overall HPP controller regulating the plant's response.
- Utilise forecast data for power balance under normal operation and observe the impact of different battery capacities.
- Implement primary and secondary frequency responses based on standards.

- Monitor the spot price of the power market to analyse the economic aspect of the negative spot price on curtailment and market participation.

1.2 Limitations

- Aggregated models for WTs and PVs are used and individual unit dynamics are not evaluated.
- Inverter details and Pulse-width modulation (PWM) are not considered in modelling for simplification.
- Since the project is limited to active power regulation, the concepts of voltage stability, reactive power compensation and fault tolerance are not included.
- Battery lifetime considerations and degradation are not considered a part of the project.
- Computational delays have not been taken into account.
- The calculation of ramp rates is not included in this project.
- The setpoint for AS considered in the controllers is based on frequency deviation and not on power setpoint. In real scenarios, the power delivered is set at a particular value. This is done to simulate the behaviour of secondary response on the frequency.
- The findings of the project do not include inertial response.
- Effect on power quality such as harmonics are neglected.
- Limited market conditions as stated are taken into account for investigation.

1.3 Methodology

This project focuses on active power regulation for frequency support through an HPP. In this project, a HPP is modelled in DigSILENT PowerFactory with generation units WTs and a PV park connected to batteries as storage units. The total installed generation capacity of the plant is at 65.65 MW and the battery's capacity is varied according to the services provided in each test case. The storage unit is modelled using a static generator to both absorb and provide power according to the system's needs. The plant is connected to the distribution grid at 63 kV connection busbar. The external grid is modelled as a combination of the PowerFactory external grid model and an external load with 50 MW capacity. The simulated model is a hypothetical scenario created in collaboration with Eurowind Energy.

The generation units receive real production data through a Digsilent Simulation Language (DSL) model of a dispatch controller based on the market spot price. An HPP

controller is modelled using DSL tool in PowerFactory for controlling the active power output of the HPP to provide different services, as stated in the objective. During forecast matching, the deviation between the forecasted production and actual production creates the Battery Energy Storage System (BESS) power reference. When the HPP is required to provide AS the frequency deviations of the system and the control modes determine the generated reference. The BESS controller modelled as DSL model is used to control the battery output power based on the reference from HPP controller. This implies that the BESS controller is calculating the required battery power both for charging and discharging purposes based on the developed Battery Management System (BMS).

The above system is modelled and tested to verify the correct behaviour of the HPP plant. Different test cases are simulated to further study how the active power is regulated during various events that affect the system's frequency. Events considered are production variations due to forecast mismatch, AS due to load variations, and an economic scenario related to production curtailment during negative spot price in the market. Through these test cases, the requirements from grid codes and tender conditions are analysed to ensure the fulfilment of these terms as well as provide an economic view.

1.4 Chapter Structures

In this report, the chapters are structured as follows.

The first chapter gives a short introduction to the relevant background on HPP and storage technologies. Moreover, it introduces the problem this project deals with and why this is important along with the project objective, tasks and limitations. Then, the methodology is described.

The second chapter describes the basic principles of frequency stability, active power regulation, grid codes, electricity market, frequency ancillary services, HPP configurations, and controllers' architectures from the existing literature related to this project.

Chapter three provides a description of the modelled system. Both the system components and their controllers are described with the necessary details for understanding the operation and capabilities of the HPP.

Thereafter, the fourth chapter presents the simulated test cases along with the results, observations and conclusions of each implementation. The test cases included in this project are forecast production matching with actual production, provision of frequency AS and the effect of spot price.

In the fifth chapter, the important discussions of the project are elaborated.

Following this in the sixth chapter, the overall project conclusions are then examined in

1. Introduction

light of the outcomes that were attained.

The seventh chapter includes the suggested beneficial future work for this project.

2 State of the Art

In this chapter, an overview of the state of the art that is relevant for this project is presented. This includes the power system challenges related to the frequency and its relation with the active power along with descriptions of selected active power regulations that are provided to the grid through support services. Then, the electricity market is briefly explained. Thereafter, the different ways of designing an HPP are mentioned with its different components. This is followed by a specific control architecture that will be dealt with in this project.

2.1 Power System Frequency Challenges

With higher penetration of RES technologies and Inverter Based Resources (IBRs) in the power system, the system inertia declines affecting the grid frequency. This frequency signifies the power generation and load demand balance and needs to be maintained within the operational limits determined by TSOs. [8]

The frequency excursion in a power system during a disturbance at 0 s is illustrated in Figure 2.1. The frequency drop from its rated value and the Rate of Change of Frequency (RoCoF) are observed. Frequency reaches a minimum value called frequency nadir which is restricted by the inertial response. Through the provision of the different reserves, the frequency increases to reach the nominal value and stabilise. The reserves are applied through different controls. At first, the primary control is applied, in the time frame starting from 0 s and continuing up to 15 mins after the disturbance, to bring generation and load in balance and keep the frequency close to its nominal value [9]. Within 30 s the secondary response is activated to restore the frequency to its nominal value and release the primary response. At last, the tertiary response is applied when the secondary control is insufficient and releases the secondary reserves resulting in a balanced system. [10], [11]

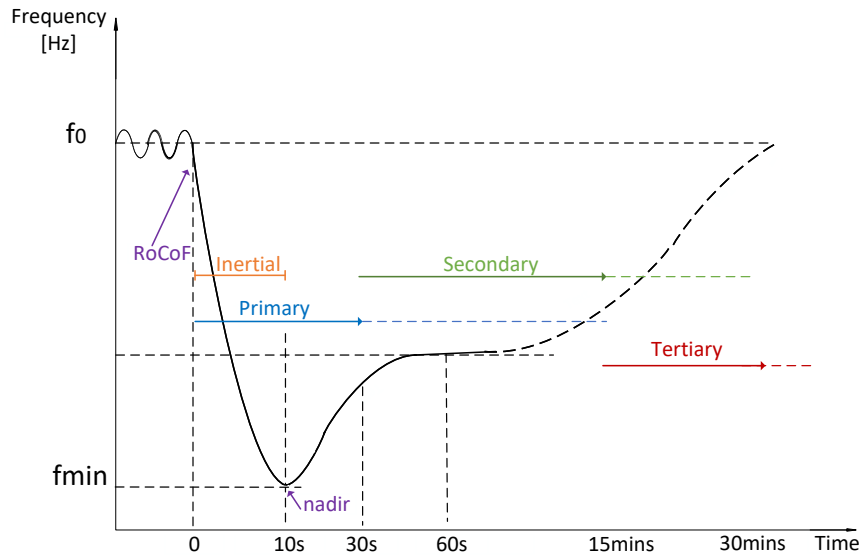


Figure 2.1: Frequency excursion during a disturbance [12].

2.2 Active Power Regulation

One way to fulfill the frequency requirements is by controlling active power. Active power is related to frequency, based on Equation 2.1, therefore, when there is an unbalance in active power, frequency changes. Thus, by accomplishing active power regulation the frequency changes can be controlled. Hence, in case of under-frequency, that is when the frequency drops below the limits, an increase in generated power is required and active power needs to be injected into the grid and vice-versa for an over-frequency event. [13]

Furthermore, based on the type of generation unit, when the frequency changes and the primary response is active, the droop (R) in the generators is activated determining the frequency change over the power change. The droop percentage is defined as the percentage of frequency change over the power change percentage as stated in Equation 2.1 [14].

$$R[\%] = \frac{\text{frequency change}[\%]}{\text{power change}[\%]} \cdot 100 \quad (2.1)$$

The default modes for active power regulation in HPPs and RES are stated in Table 2.1 [15]. The Limited Frequency Sensitive Mode—Underfrequency (LFSM-U) corresponds to upward regulation when frequency is below the threshold limit f_{RU} and Limited Frequency Sensitive Mode—Overfrequency (LFSM-O) for downward regulation above f_{RO} , while Frequency Sensitive Mode (FSM) is active to stabilise the system's frequency within

the mentioned range. The grid codes for Denmark are divided into two categories depending on the covered area. DK2 is for Eastern Denmark, which is synchronised with the Nordic Grid and for Western Denmark, it is DK1 connected to the Union for the Co-ordination of Transmission of Electricity (UCTE) [16]. The grid codes for the DK1 area are mainly considered in this project.

Table 2.1: Grid code settings in DK1 for LFSM-U, LFSM-O and FSM [17], [15].

Mode	Characteristic	Specification for DK1
LFSM-U	Frequency limit f_{RU}	49.8 Hz
	Frequency control range	47.5 Hz to 49.8 Hz
	Droop	5%
LFSM-O	Frequency limit f_{RO}	50.2 Hz
	Frequency control range	50.2 Hz to 51.5 Hz
	Droop	5%
FSM	Frequency control range	49.8 Hz to 50.2 Hz
	Droop	2-12%
	Dead band	± 20 mHz
	Control Insensitivity	± 10 mHz

Figure 2.2 illustrates the ranges for the control modes based on their droop characteristics and specifications.

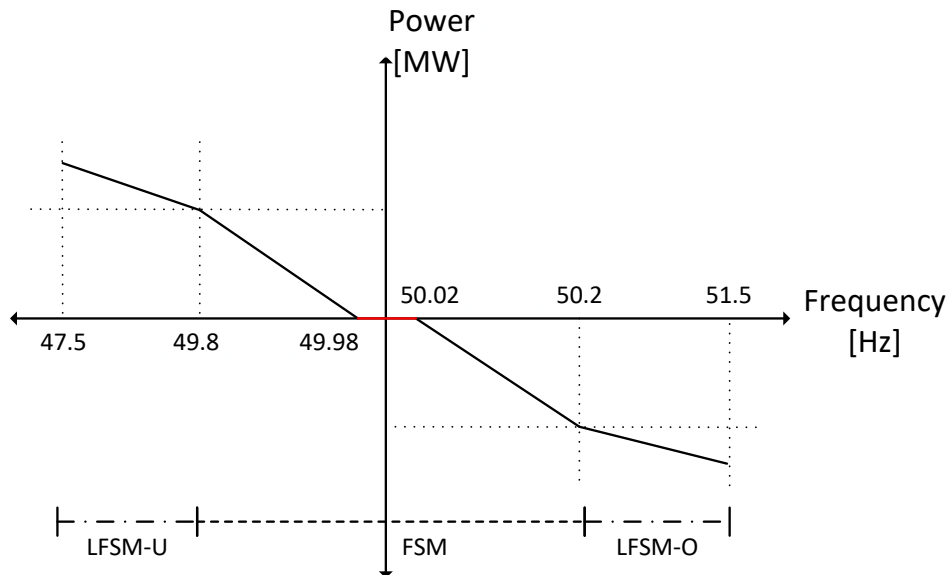


Figure 2.2: P/f droop characteristics of the control modes.

2.2.1 System Frequency Requirements

The technical specifications such as grid codes and tender conditions for Denmark are set by Energinet as stated in Table 2.2 to make certain that the system will operate safely.

Based on [16], the allowed frequency deviation is ± 200 mHz for a system frequency of 50 Hz. The RoCoF can vary no more than ± 2 Hz/s for the whole system. The ramp rate indicates the maximum speed of change of the active power. For upward and downward regulation, it can reach values of up to 20% of the installed capacity per minute and a minimum of 1% [15]. Also, there is the possibility for the plant to disconnect in case the RoCoF is higher than ± 2.5 Hz/s for a duration longer than 80 ms, based on the protection relay settings [18].

Table 2.2: System frequency requirements [16], [15].

Parameter	Specifications
Frequency Deviation	± 200 mHz
Frequency Deadband	± 20 mHz
RoCoF	± 2 Hz/s
Ramp Rate	max. 20%, not exceeding 60 MW/min min. 1%

2.3 Electricity Market

In Denmark, it is a competitive market for trading electricity, while monopolies own the transmission and distribution grids. The market is divided into wholesale and retail. Day-ahead, intraday and AS markets are part of the wholesale market and retail market provides to the consumers [19]. The trading of electricity is done by the suppliers and the Balance Responsible Party (BRP)s. A BRP is defined by Energinet as "A player approved by and party to an agreement with Energinet.dk regarding assumption of responsibility between notification and actual consumption/production at a number of metering points" [20]. TSOs of Finland, Sweden, Norway, Denmark, Estonia, Latvia and Lithuania have a free trading platform for the electricity market called **Nord Pool Spot**. BRPs trade electricity on Nord Pool every day for the next 24 hours based on forecasting of production and consumption. In case of a mismatch between the forecasted and actual values, the difference is regulated by Energinet through the **Balancing Market** and the **Ancillary Service Market**. BRPs responsible for the imbalances bear the cost of the services. [21]

The biddings with lower prices than the market clearance price get accepted, considering that they fulfil the TSO's technical requirements. Also, the prices differ according to the bidding hours. For instance, for a particular day during peak hours in DK1 (8:00-20:00), the bidding can reach approximately 73€/MWh for this block, while for off-peak times such as 20:00-00:00 the price can be around 69€/MWh. These prices can vary depending

on the market conditions. [22]

Based on Energinet tender conditions for AS, the bids for primary reserve need to be given with a price and quantity for a 4-hour block per MW. Six 4-hour blocks divide the 24 hours in a day. As per requirement, the minimum bid that can be stated is 1 MW. For secondary reserve there is also an upper limit for maximum 50 MW. However, the AS market bidding time is also defined by the services. An example is that the secondary reserve has weekly bidding and not hourly like the primary reserve. [16]

More information for AS requirements can be found in [16].

2.4 Frequency Ancillary Services

The different services that can be provided are separated based on their reserve purpose and time duration. For frequency control services and for primary response Fast Frequency Response (FFR) and Frequency Containment Reserves (FCR) services are applied. For secondary response the Frequency Restoration Reserves (FRR) service exists and for tertiary support, the Replacement Reserves (RR) is implemented. The purpose and duration time for these services are listed in the following Table 2.3, based on [16], [8], [23].

Table 2.3: Ancillary services requirements [16], [8], [23].

Service	Purpose	Activation Time
FFR	re-strain the RoCoF in the system	up to 0.7 s
FCR	regulate frequency close to nominal frequency	up to 2 s, 15 s first half, 30 s second half
FRR	return frequency to nominal frequency	supply full reserve by 15 mins
RR	bring back the status of operating reserves	mins to hours

In addition to the above table and corresponding to the frequency excursion Figure 2.1, in Figure 2.3 the time frame of the services can be observed with one releasing the previous service during that period. Moreover, FFR has negligible energy delivery during the service, while the FRR requires higher energy delivery.

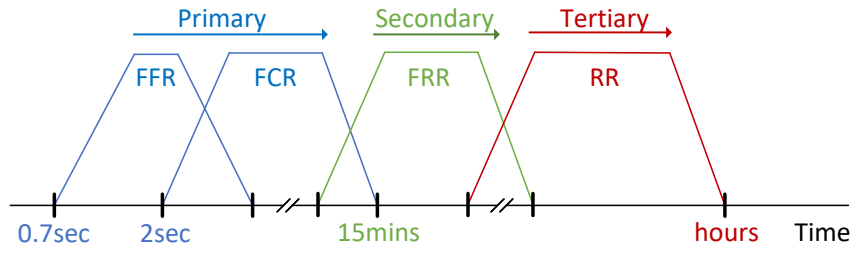


Figure 2.3: Time frame for ancillary services [9], [16].

Furthermore, these services are also categorized based on the way they are activated. For instance, the FCR is only activated automatically taking into consideration the frequency measurements on the local power plants. It can also be divided into Frequency Containment Reserve for Normal Operation (FCR-N) and Frequency Containment Reserve for Disturbances (FCR-D) based on the grid codes of DK2. Normal operation is considered to be within the frequency range of $50 \pm 1\text{Hz}$, while disturbances are considered to occur below 49.9 Hz and above 50.1 Hz. Also, FFR is an automatic response service considered a type of synthetic inertia responding to frequency fluctuations. On the other hand, FRR has both automatic and manual control with the manual taking longer response time of 15 mins while the automatic one response within 2 mins. [8]

The TSOs choose if the generator is suitable to provide services according to its online situation, the availability of the unit and their impact on the system. Because of the markets for these services, the bid needs to be accepted before the service is activated [24].

More details on the different AS can also be found in [24].

2.5 HPP Configurations

Different hybrid plant structures can be installed depending on their purpose. The focus of this project is on renewable units like WTs and PVs with batteries for storage.

When HPPs depend on WTs to provide a reserve, they have to operate below their Maximum Power Point (MPP) to ensure an overhead for power generation. This limitation introduces the need for storage methods in such HPPs to provide the necessary reserve. Also, during peak production hours, the HPPs are required to curtail their production as required by the TSO. This curtailed excess power can be used as stored energy and act as reserves for support services to the grid. [25]

The WTs can have an AC or a DC coupling depending on the specification of a project, connection with storage, the grid services, along with the existing market prices [26]. The following options exist which are illustrated in Figure 2.4. Firstly, one way is to connect

the PV park with the batteries in a DC bus shown in Figure 2.4a, which is an available topology in the industry and is also used for residential applications. The second configuration Figure 2.4b, is an AC coupled where all aggregated components are connected at the Point of Common Coupling (PCC). This topology has an advantage because it can be designed and developed in a more independent way where the BESS size doesn't depend on the PV converter rating. The last topology that is illustrated in Figure 2.4c, is the one that has all the aggregated components coupled in a DC bus and then through an inverter connected to the PCC. Typically, the PV and BESS coupling depends on whether the produced solar power is used for supply or only for storage. [27]

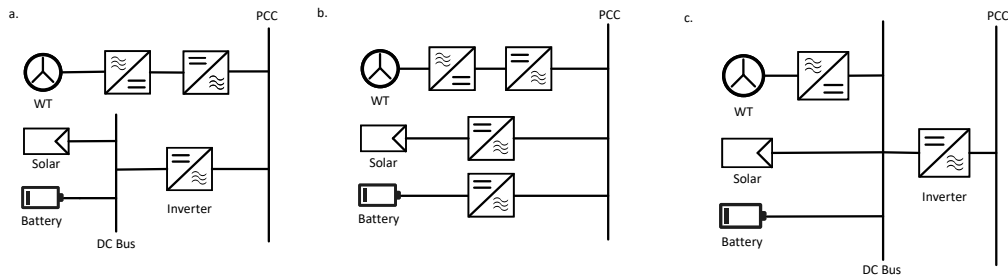


Figure 2.4: HPP configurations, a) DC coupled PV and BESS, b) AC coupled, c) DC coupled [27].

Energy Storage Methods

Various energy storage methods have been developed to store energy and use it when required. The majority of them have a name that refers to the form that the energy is stored such as chemical, thermal, mechanical, and electrical storage technologies. While electrochemical indicates the reaction type on which the batteries are based on. Based on [28] the methods are briefly explained below.

Chemical Method: Chemical storage technologies store energy as chemical bonds. The basic principle of electrolysis is that hydrogen gas production is accomplished from water using electricity. With the addition of chemical compounds, hydrogen can be modified into other forms making it easier to store and transport. Hydrogen technology has the potential to use already existing gas networks with high energy density but it requires compression to reach enough energy density. Furthermore, the efficiency for electrification is lower than 40%, and the investment costs for electrolyzers are high.

Thermal Method: Thermal methods store the energy in the form of heat. There are different types of energy thermal storage which have to do with the physical state of the material that is heated. Firstly, there is the sensible heat where the material remains unchanged. Then, there is the latent heat which is associated with the phase change of a material and at last, the thermochemical heat that consumes or releases thermal energy

with an opposite reaction. These technologies have high discharge durations.

Mechanical Method: Mechanical methods are related to energy storage in the form of gravitation, compression, and linear or rotational motion. For these technologies electric generators, motors, pumps and turbines are used to convert the energy from electrical to mechanical. In the case of pumped hydro systems while the lifetime is long, there is the need for suitable geographical conditions, long construction time, and long discharge duration that can be more than four hours.

Electrical Method: For this method, capacitors and inductors are used. The energy is stored in the electric field between the conductive plates that are separated into positive and negative charges through capacitance. In the case of inductance, the energy is stored as current flowing through a coil with the use of a magnetic field generated from the same current. Superconductors have high power density ($100\,000\text{ kW/m}^3$) while the energy density is low (20 kWh/m^3). Also, while having a high cycle life their discharge duration is short and they have high energy cost.

Electrochemical Method: Electrochemical reactions happen inside the batteries where energy is stored as electrochemical potential between two materials. It can have a solid state electrolyte, e.g. Li-ion or a liquid electrolyte, e.g. Flow batteries. In lithium-ion batteries e.g. Li-Iodide, the chemical energy from the separation of the lithium (Li) and Iodine (I_2) in a solid electrolyte is converted into electrical energy during discharge as electrons travel from lithium anode to iodine cathode as illustrated in Figure 2.5.

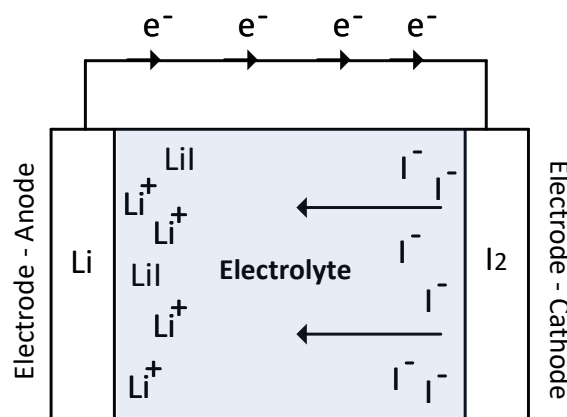


Figure 2.5: Lithium iodine batteries [28].

For Lithium-ion battery there are safety risks because of thermal runaway and degradation throughout the operational lifetime. Also, the cycle life is limited to approximately 3.500 at 80% depth of discharge. However, they have high efficiency of upto 85%, high

energy densities (450 kWh/m^3) and power densities (6000 kW/m^3), fast response time, less than one second and their cost is reduced because of the variety of markets. [28]

BESS are also becoming popular because they can support the grid continuously when there are high load demands, provide frequency regulation, and support transmission problems. To accomplish the required output power the voltage and current of the battery are designed by organizing the battery modules. In case an increase in voltage output is desired then the battery packs are series connected and in parallel when current increase is wanted. Furthermore, batteries are dynamic systems and because of their cycling operating behaviour, the packs degrade with time. Degradation is affected especially when they are overcharged or undercharged during their charging cycles or when the temperature is extreme etc.. To minimize degradation and increase the battery's life, its operation needs to be optimally designed. [8].

Due to their fast response time, BESS can be used to provide primary control services and improve the system's reliability by having the ability to react immediately after a contingency. BESS can respond to frequency deviation within milliseconds ramping up from 0 MW to full load. Secondary and tertiary frequency control reserves can be limited based on the storage available in the battery. These reserves require larger units. [29]

Based on the aforementioned, batteries can be used for storage as they can provide a very fast response time and have the possibility to comply with the requirements related to support services [8]. In addition, the batteries can be connected with the PV plant due to the fact that the PV panels can not produce any power in the night hours and the battery can complement the needs that might occur in that time. The WTs can operate at all times as long as there is wind [30].

Implementation of storage with PV plants has four different configurations based on their operating purposes according to [30]. First, there is the option of connection without a PCC as illustrated in Figure 2.6a. Then, there is the configuration with only AC coupled bus, shown in Figure 2.6b. Bi-directional inverter is included for the BESS in these topologies. The other option in Figure 2.6c, is to have DC coupled with a common bi-directional inverter where the charging is flexible. These configurations can store electricity either from both the grid and the PV or only the PV based on their structure and have an integrated inverter and BMS. [30]

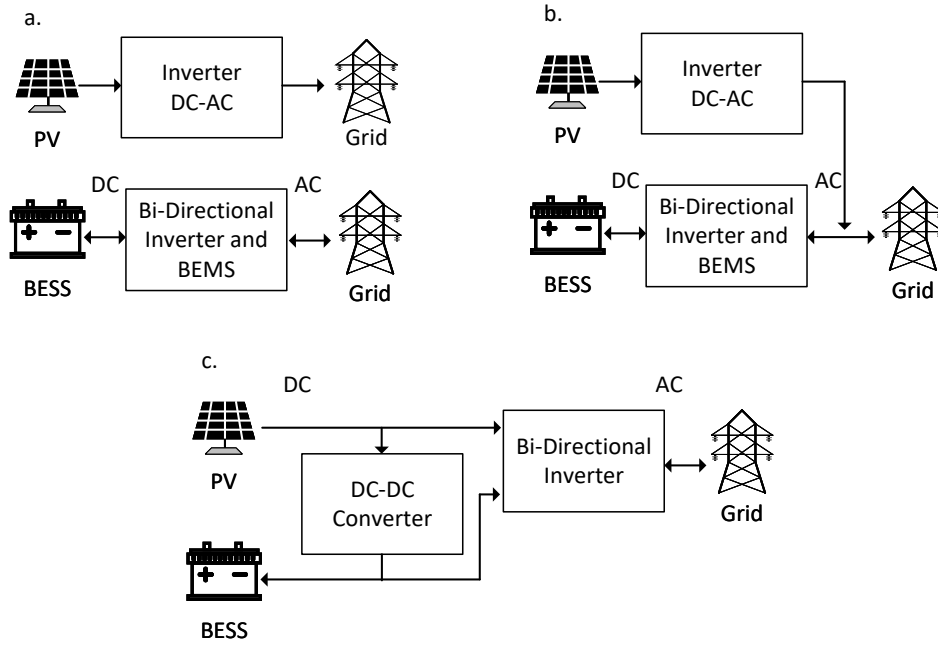


Figure 2.6: PV with BESS configurations, a) without PCC, b) only AC coupled bus, c) DC coupled with a common bi-directional inverter [30].

2.6 Controller Architectures

The HPPs consisting of only RES rely on different converters and control architectures for the operation of the IBRs. The fully controlled IBRs in the power system are connected to the Point of Connection (PoC) or the PCC through Machine Side Converter (MSC) and Grid Side Converter (GSC) as shown in Figure 2.7. The MSC is determined by the dynamics requirement of the particular resource while the GSC determines whether the resource is in Grid Following (GFL) or Grid Forming (GFM) mode. The MSC controller aims to operate at MPP. The AC power and the DC link voltage are maintained by the control of GSC. The controllers have inner loops for voltage and current and outer loops for active and reactive power. The inner control loop parameters are used to generate the PWM signals for the converter control. The grid side Low-pass filter (LPF) is used to reduce the effect of harmonics due to the PWM in the GSC. The types of GSCs implemented in this project is the Voltage Source Converter (VSC). Some of the relevant topics related to the VSCs being dealt in this project are briefly described in the following subsections including the frequency-dependent active power control. [31]

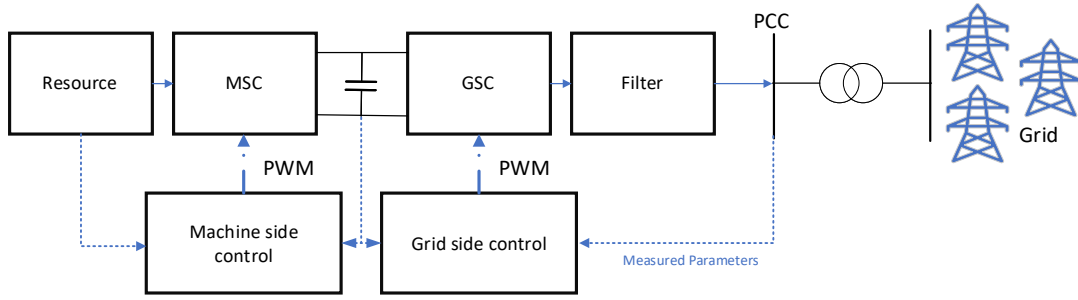


Figure 2.7: Inverter based resource architecture [31].

2.6.1 Grid Following Mode

As mentioned above, the GSC or VSC can operate on different modes. In GFM mode, the converter output follows the grid parameters i.e. the voltage generated by the VSC is synchronised to the grid voltage and grid frequency. A Phase Locked Loop (PLL) is implemented to lock the VSC output voltage to the grid voltage at a phase angle. Figure 2.8 shows the equivalent model of the VSC. The power exchange between the VSC and the grid can be described by the Equations 2.2, 2.3 from the phasor representations shown in Figure 2.9. [31]

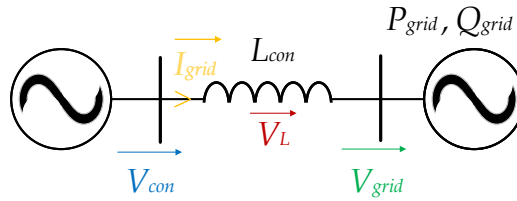


Figure 2.8: Equivalent model of grid connected VSC [31].

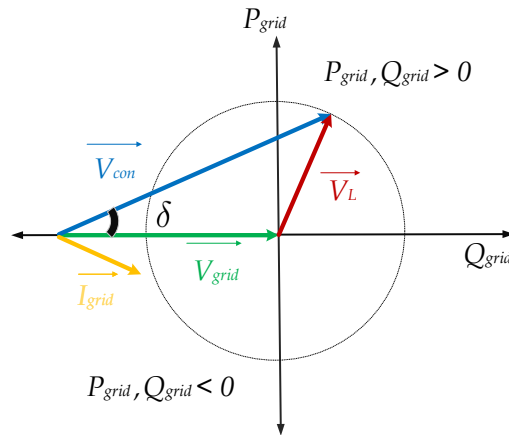


Figure 2.9: Voltage and current phasors [31].

$$P_g = \frac{V_{con} V_g}{X_L} \sin \delta \quad (2.2)$$

$$Q_g = \frac{V_g}{X_L} (V_{con} \cos \delta - V_g) \quad (2.3)$$

When $\delta \approx 0$, $P \propto \delta$ or $P \propto f$ and $Q \propto \Delta V$. [31]

These inter-dependencies of the parameters P and Q on δ and ΔV are implemented in the control loops to control the VSC to derive the required active and reactive power that needs to be transferred into the grid and also to maintain the voltage at the PCC.

2.6.2 Current Control of VSC

The 3-phase grid connection of VSC is given by the Figure 2.10 and the Equation 2.4 is obtained using Kirchhoff's Voltage Law (KVL).

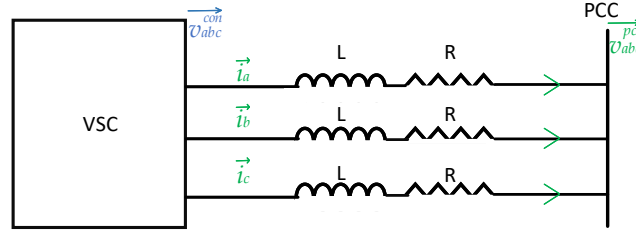


Figure 2.10: Simplified circuit of 3-ph grid connection of VSC [31].

$$\begin{bmatrix} v_a^{con} \\ v_b^{con} \\ v_c^{con} \end{bmatrix} - \begin{bmatrix} v_a^{pcc} \\ v_b^{pcc} \\ v_c^{pcc} \end{bmatrix} = \begin{bmatrix} R & 0 & 0 \\ 0 & R & 0 \\ 0 & 0 & R \end{bmatrix} \begin{bmatrix} i_a \\ i_b \\ i_c \end{bmatrix} + \begin{bmatrix} L & 0 & 0 \\ 0 & L & 0 \\ 0 & 0 & L \end{bmatrix} \frac{d}{dt} \begin{bmatrix} i_a \\ i_b \\ i_c \end{bmatrix} \quad (2.4)$$

The above equation can be converted to the synchronous reference frame by Equation 2.5 using Park's transformation.

$$\begin{bmatrix} v_d^{con} \\ v_q^{con} \\ v_0^{con} \end{bmatrix} - \begin{bmatrix} v_d^{pcc} \\ v_q^{pcc} \\ v_0^{pcc} \end{bmatrix} = \begin{bmatrix} R & 0 & 0 \\ 0 & R & 0 \\ 0 & 0 & R \end{bmatrix} \begin{bmatrix} i_d \\ i_q \\ i_0 \end{bmatrix} + \begin{bmatrix} L & 0 & 0 \\ 0 & L & 0 \\ 0 & 0 & L \end{bmatrix} \frac{d}{dt} \begin{bmatrix} i_d \\ i_q \\ i_0 \end{bmatrix} + \omega \begin{bmatrix} L & 0 & 0 \\ 0 & L & 0 \\ 0 & 0 & L \end{bmatrix} \begin{bmatrix} -i_q \\ i_d \\ i_0 \end{bmatrix} \quad (2.5)$$

Equation 2.5 is used for current control of the VSCs as shown in Figure 2.11. The zero sequence component is neglected due to its absence in a balanced 3-phase system.

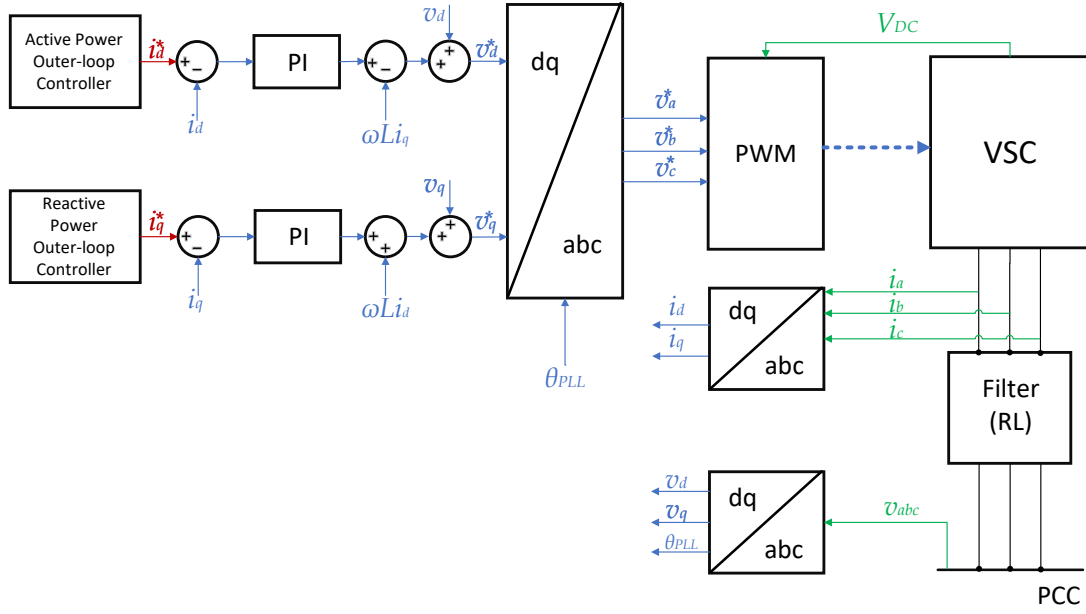


Figure 2.11: Current control architecture of VSC [31].

P and Q loops are the outer active and reactive power control loops. These are based on the power requirement at the PCC and provide the setpoints or reference values i_d^* and i_q^* for i_d and i_q current components, respectively. The PI controller present in the inner current control loops ensures that the dq-current values reach the setpoints i_d^* and i_q^* . Feed-forward terms v_d , v_q and decoupling terms $-\omega L i_q$, $\omega L i_d$ as seen in the Equation 2.5 is used to generate the required voltage setpoints v_d^* and v_q^* for the VSC. [31]

2.6.3 PQ control loop

The instantaneous active and reactive power transferred by the VSC in dq-frame is given by Equations 2.6 and 2.7.

$$P = \frac{3}{2}(v_d i_d + v_q i_q) \quad (2.6)$$

$$Q = \frac{3}{2}(v_q i_d - v_d i_q) \quad (2.7)$$

When the VSC is synchronised to the grid using the PLL, the v_d is aligned to the grid voltage and $v_q = 0$. This leads to the Equations 2.8 and 2.9.

$$P = \frac{3}{2}v_d i_d \quad (2.8)$$

$$Q = -\frac{3}{2}v_d i_q \quad (2.9)$$

Based on the above equations, Figure 2.12 shows the outer PQ-control loop for generating the reference current signals i_d^* and i_q^* for the inner control loops based on the PQ requirement at the PCC i.e. P_{ref} and Q_{ref} . [31]

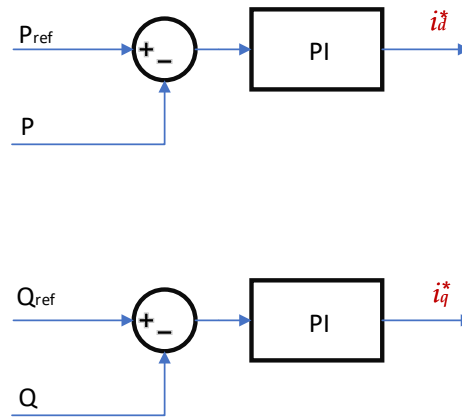


Figure 2.12: PQ control architecture of VSC [31].

2.7 Chapter Summary

First, the frequency is an important factor that creates challenges to TSOs in order to balance the supply and demand. For this reason, they set requirements that all participants have to follow for the system to stay reliable and balanced. To tackle the unbalances that might occur during the day, there are ways to regulate the active power and improve the frequency response. This is accomplished through Ancillary Services that plant owners can provide to the grid, creating electricity market opportunities. These services differ by their supply time and their requirements. Furthermore, HPPs have different possible structures depending on how their components are coupled and their purpose of installation. The architecture can be more detailed when it comes to the PV and BESS coupling mostly because of the inverters. Finally, in an HPP the controllers determine the plant's operation both under normal operation and also in case it has to respond to a disturbance in the grid and provide its support to balance it. Different architectures are described in order to understand their use and design.

3 System Description and Modelling

In this chapter, the system that is modelled is described. After an overview of the plant, detailed modelling for the system is provided. Also, the controllers implemented in the HPP are further explained for a better understanding of the plant's functionalities and capabilities.

3.1 System Description

In this project, the system that is examined is a hybrid power plant, which indicates that the RES technologies are connected in the same PCC. The generation sources of interest are WTs and PVs with batteries as a storage unit.

The system configuration is illustrated in Figure 3.1. It is modelled in PowerFactory Software and DSL is used to develop the different controllers.

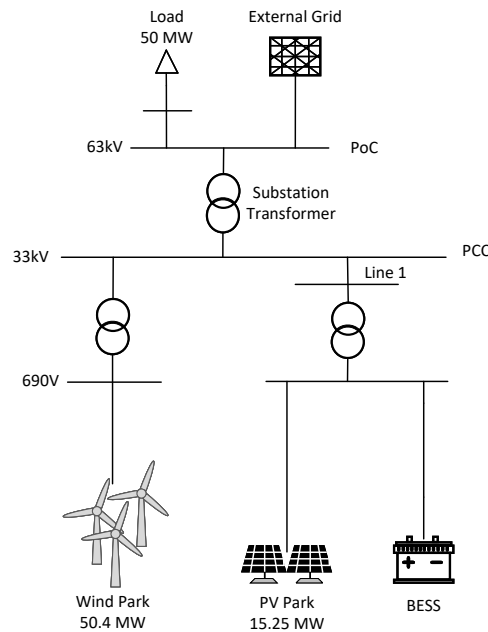


Figure 3.1: HPP overview.

A power factor equal to one is used, to ideally consider only the active power flow. The PV park and BESS are connected in an AC bus to store either solar power when possible or absorb grid power when required. As shown in Figure 3.1, the units of the plant are connected to a PCC bus at 33 kV and then with a substation transformer at the PoC of 63 kV, with the external grid and a load of 50 MW.

3.2 System Modelling

3.2.1 Wind and PV Generation Units

The wind farm is modelled as an aggregated model of 50.4 MVA for twelve, 4.2 MW Vestas V136-4.2MW wind turbines [32], [17]. The PV park is also modelled as an aggregated model with a central inverter. The park's rated apparent power is at 15.25 MVA to match the active power for the total capacity. These plant capacities are based on the actual data provided for the project.

The production data of the units is provided as confidential data from real hybrid power plants and is imported with the use of DSL models in the dispatch controller which is explained in Section 3.3.2. Slots are used to read the measurement files and import them to the plant elements. The production profiles differ according to the test cases and details are provided in the description of the individual test cases.

3.2.2 Battery

The BESS is modelled by a static generator to mimic a VSC. The inputs to the static generator are the voltage setpoints v_d^* and v_q^* . These signals are generated from the BESS controller to provide the required power output. The output power provided is based on the rating of the static generator, $Prated$, which signifies the converter/battery power rating. Sizing parameters for the BESS are based on the conditions of each test case.

3.2.3 External Grid

The grid is represented by external grid component in PowerFactory. It has a secondary frequency bias of 10 MW/Hz to balance the active power to some extent and provide some secondary reserves [33]. The acceleration time constant is set to be 10 s since the goal is to be able to observe frequency variations based on the modelled HPP as it represents the total inertia in the external grid [34]. The inertia constant of the external grid is assumed to be 5 s to behave as a synchronous generator (thermal unit), which results in the considered value of the acceleration time constant [35]. The short circuit ratio and the X/R values are provided as confidential data. In addition, a controllable load of 50 MW default value, is connected to simulate different frequency events therefore its default value is modified accordingly.

3.2.4 Transformers and Transmission Line

The substation transformer data was provided by the plant owners with its parameters stated in Table A.1 in Appendix A.1. [17]

The generation units are connected to transformers with rated voltage of 0.69/33kV and their rated power is modified to respond to the system requirements. [17]

In the system, there is only one underground cable line connecting the PV park and battery to the PCC. Its aggregated parameters are stated in Table A.2 in Appendix A.2. Short cable lines are neglected. [17]

3.3 System Controllers

3.3.1 HPP Controller Architecture

This subsection describes the overall modelling of the HPP controller, where all the Distributed Energy Resources (DERs) are connected to a common controller. The HPP controller is modelled as a composite DSL model which communicates with WT, PV and BESS Controller as per the service.

The calculated power $P_{Bessref}$ in p.u. that should be provided to the battery will be the output signal from the HPP controller, either from the power mismatch calculation or from the frequency controller in case of a frequency deviation. In Figure 3.2 the structure of the HPP controller is illustrated. The forecasted data are imported as measurement files for both PV and wind. The actual plant production from RES is measured. The PLL is measuring the grid frequency, cosphi and sinphi at the PoC bus which will be further used and the battery power is measured at the BESS bus.

The HPP controller has the capability to calculate the power mismatch between the forecasted production data and the actual production of the plant. The power mismatch is calculated based on Equation 3.1 and it will be provided/absorbed by the BESS to complement the expected power values. This action will be activated in case the market goal is to provide the promised forecasted power when the grid operates under normal conditions. This is enabled by the *Enable Key*.

$$Power\ mismatch[p.u.] = \frac{(PV_{forecast} + WT_{forecast}) - (P_{WTProduction} + P_{PVProduction})}{P_{BESSnominal}} \quad (3.1)$$

3. System Description and Modelling

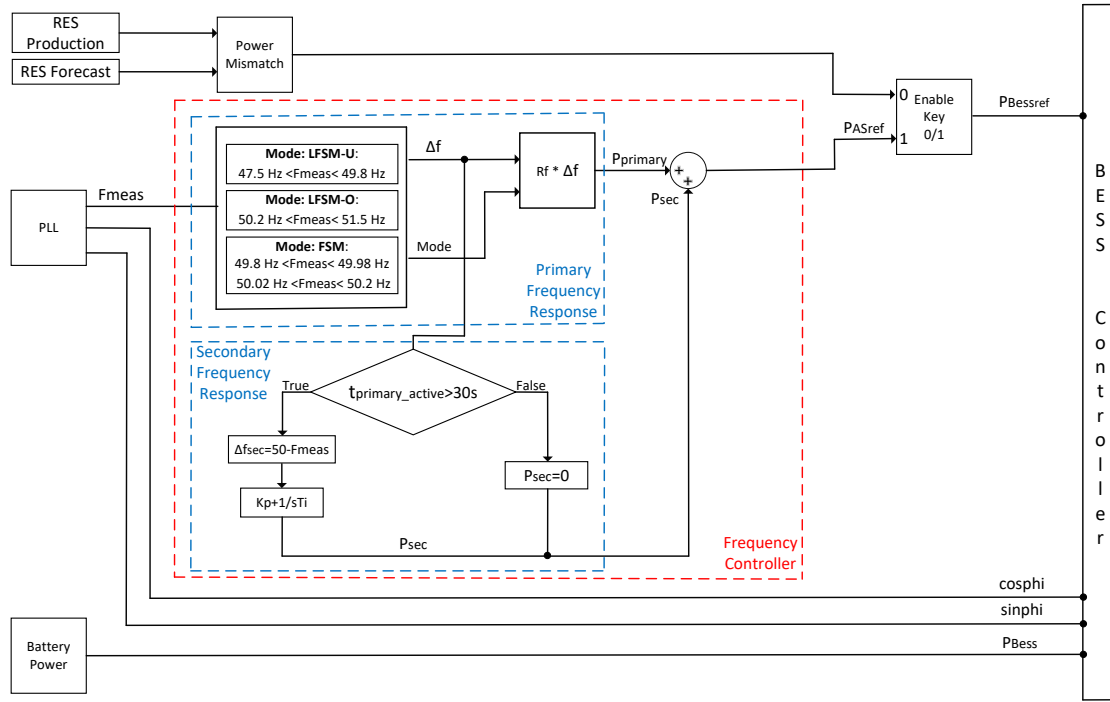


Figure 3.2: HPP controller architecture.

When the plant operates to provide the frequency AS, the active power reference value P_{ASref} is generated by the BESS controller to regulate the active power requirement of the grid based on the change in frequency Δf with respect to the nominal frequency f_n . The different frequency control modes and the different services specifically determine this value. These calculations are executed inside the frequency controller which is further analysed below.

Frequency Control Implementation

The frequency control is implemented as a composite model where the power reference for the battery is calculated in case of frequency deviation as shown in Figure 3.2. It is designed to provide a power signal including both primary and secondary frequency responses. The details of the individual responses are described separately in the next sections.

Primary Response:

The primary response is initiated through the selection of the frequency control mode that will get activated based on the frequency range and default droop values indicated in Table 2.1. The code implemented considers the characteristics illustrated in Figure 2.2 based on the droop gain $R_f = 1/\text{Droop}$, according to the frequency modes. FSM and LFSM-O/LFSM-U model implementation are described below. The mode droops can vary based on the required active power [36].

3. System Description and Modelling

The FSM mode is implemented in the frequency range of 49.8 Hz to 50.2 Hz with a ± 20 mHz deadband around the nominal frequency 50 Hz. These values are based on the Danish grid codes described in the state-of-the-art. The power calculation in p.u. ($P_{f_{sm}pu}$) based on the droop gain ($Rf_{f_{sm}}$) for this frequency range is given by Equation 3.2, where $\Delta f_{f_{sm}}$ is the deviation in frequency within FSM frequency limits from the nominal frequency f_n [37]. After this range, the power attains a saturation value.

$$P_{f_{sm}pu} = Rf_{f_{sm}} \cdot \frac{\Delta f_{f_{sm}}}{f_n} \quad (3.2)$$

This Equation 3.2 is represented by the yellow dotted plot without dead-band in Figure 3.3.

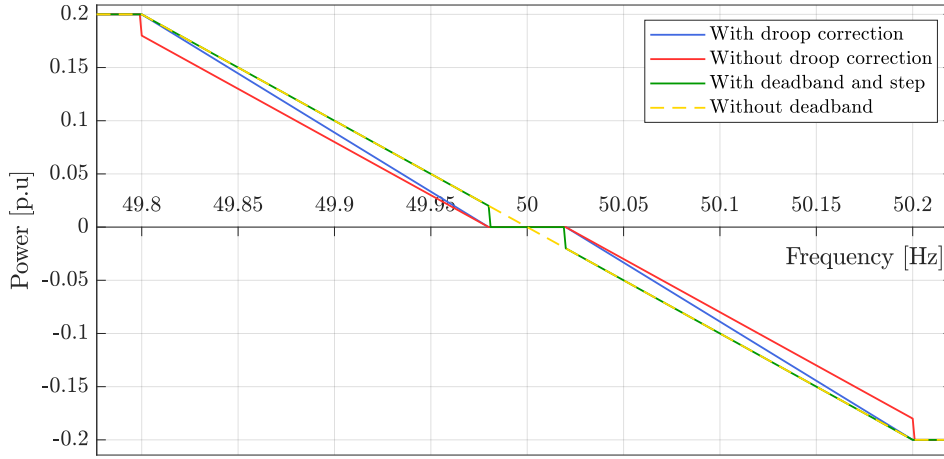


Figure 3.3: FSM droop characteristics.

The same equation when implemented with deadband yields the green plot in the figure. This plot includes a step at 49.98 Hz and 50.02 Hz i.e. the lower and upper limits of the deadband. Deadband is implemented in order to prevent sensitivity of the controller to smaller frequency variations, but the presence of a step variation has an impact on the performance of the controller which may cause hunting effect. To smoothen the response as a ramp, the frequency deviation is modified into Equations 3.3, 3.4 for lower and upper deviations, and droop characteristics is shown by the red plot.

$$\Delta f_{f_{sm}} = f_{LowerDeadbandLimit} - f_{measured} \quad (3.3)$$

$$\Delta f_{f_{sm}} = f_{UpperDeadbandLimit} - f_{measured} \quad (3.4)$$

The behaviour of this droop characteristic without step shows a deficit in the power provided as compared to the other two plots. To prevent this deficit of power which should be provided according to grid codes, a correction factor is implemented for the droop gain given by Equation 3.5. This correction factor was derived by equating the power Equation 3.2 with the modified power equation with Δf from Equation 3.3 for the range

3. System Description and Modelling

based on Table 2.1 for Danish networks. The value of this factor will vary according to the frequency limits specified by the relevant TSO.

$$Rf_{corrected} = Rf_{fsm} \cdot 1.111 \quad (3.5)$$

This droop-corrected characteristic is given by the blue plot in the same figure and has been implemented in the project's frequency controller.

For the LFSM-O and LFSM-U mode implementation, an additional equation is implemented along with the FSM power equations stated above, given by Equation 3.6. Rf_{lfsm} is the LFSM-O/U droop gain, Δf is the frequency deviation of the network and Δf_1 is the frequency threshold of LFSM-O/U [36].

$$P_{lfsm pu} = Rf_{lfsm} \cdot \frac{\Delta f - \Delta f_1}{f_n} \quad (3.6)$$

The LFSM-O and LFSM-U are implemented along with the FSM droop characteristics to act on the frequency range of 47.5 Hz to 51.5 Hz for this project. The combined characteristics are shown in Figure 3.4 for different FSM droop values and their effect on the active power outputs. The dotted lines show the FSM mode saturation values for the particular droops.

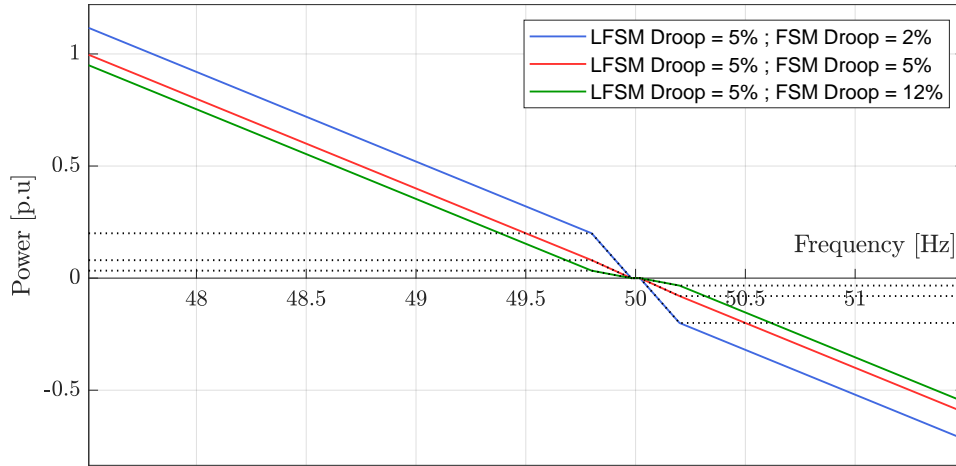


Figure 3.4: Combined P/f droop characteristics of FSM and LFSM.

The per unit power reference required to be delivered for AS by the frequency controller is based on Equation 3.7.

$$P_{ASref pu} = P_{fsm pu} + P_{lfsm pu} \quad (3.7)$$

Secondary Response:

The secondary frequency loop indicated in Figure 3.2 is modelled to respond after the initiation of primary response within 30 s using the *picdro* timer condition. Once it's activated, it passes the frequency deviation to the PI controller which in turn generates the secondary power reference P_{sec} . The PI controller has an inbuilt reset function that is used to limit the error integration in case the BESS is unable to provide the required support. This is done to increase the performance and prevent the integrator windup. More details can be found in Appendix D. The tuning parameters for the PI controller need to be based on the BESS control loops. For this reason, the values are given in Section 3.3.4 after all the controllers are introduced.

3.3.2 Dispatch Controller

A modelled dispatch controller considers the spot prices in the market and the RES production files. It has the purpose of generating an input signal $P_{SpotPrice}$ for the BESS based on the spot price and control the RES production. Firstly, a data analyser analyses the spot price from the market which is input as a measurement file for simulation purposes. The spot price values are obtained from Energinet's website [38]. When the spot price is positive then the normal operation of the plant continues, such as BESS providing the forecasted power or participating in AS and RES getting the real production data as input. If the plant operates normally and spot price is detected to be negative the battery charges with a fixed charging power from the grid in order to earn revenue, while the PV and WTs are curtailed. This charging power will be based on the converter rating with a slow charging profile to prevent adversely affecting the battery life. The reference of actual charging data is provided by the plant owners and is used for the simulation. This data is confidential and will be based on the test cases.

3.3.3 BESS Controller Architecture

The BESS controller is designed as a composite DSL model. It consists of an activation key for the negative spot price signal, the BMS, PQ and the current controller. The BESS controller model receives power reference input from the HPP controller model through a communication frame and an additional one from the dispatch controller. The inputs, outputs, and in-between computations are illustrated in Figure 3.5.

The *Activation Key* in this case determines if the BMS block will receive a power reference based on the spot price through the dispatch controller or based on the HPP controller functions. This implies that the battery can charge in total for three different scenarios. First, when the production is too high resulting in negative spot price. Secondly, when the power mismatch needs to be complemented, and lastly when the frequency has to be balanced. The individual working of the BMS and the current controller are described in the following sub-sections.

3. System Description and Modelling

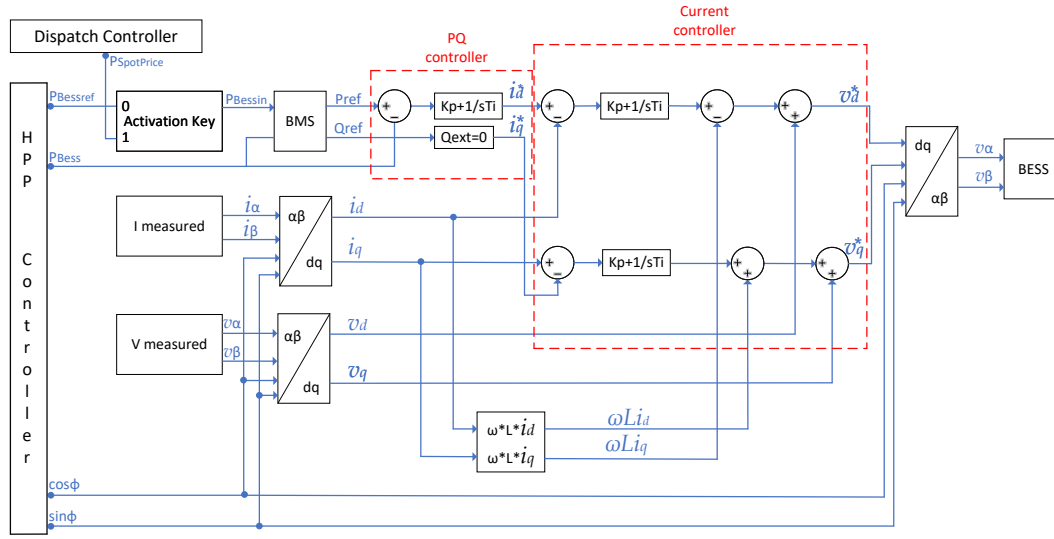


Figure 3.5: BESS controller architecture.

Battery Management System (BMS)

BMS DSL code manages the overall performance of the battery and its State of Charge (SoC). The SoC is calculated based on Coulomb counting, given by Equation 3.8.

$$SOC = SOC_0 - \frac{1}{C_{BESS}} \int_0^t I_{BESS} \cdot dt \quad (3.8)$$

BMS takes the reference power from the HPP controller as the input and based on the current SoC of the BESS decides if the required power can be provided by the BESS. The output of this block is the reference active power for the outer control loop of the current controller. The flowchart of the algorithm is shown in Figure 3.6 and the DSL code is in the Appendix E. SR-flipflop logic is used to determine the conditions for charging and discharging. According to the logic, if the set condition is true no action will take place and if the reset condition is true, the relevant action occurs. To prevent oscillations while discharging, the SoC should reach 40% before it can start discharging again. Similarly to facilitate charging, SoC must be 90% or below.

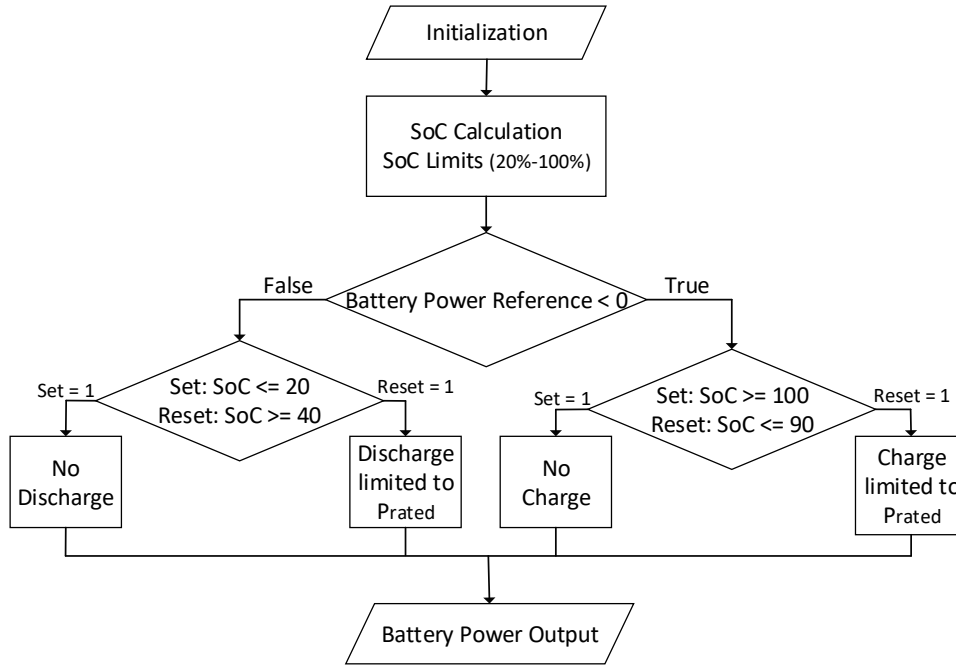


Figure 3.6: Flowchart of BMS algorithm [17].

As the BESS is modelled to behave as a VSC, the power flowing out is signed positive and the power absorbed is signed negative. The SoC is limited from 20% to 100% for better BESS life performance based on [39]. However as mentioned, the upper limit is set to 100% as compared to 80% SoC on the assumption that more lower frequency events occur than higher frequency events causing the number of full charging cycles to be lower than the number of full discharging cycles. The charging and discharging power of the BESS is limited to its converter rating (P_{rated}).

A test is performed to verify the working of the BMS in the model according to the mentioned flowchart. The behaviour of the BESS is observed in Figure 3.7, based on the step power references as shown in Table 3.1 at the corresponding times.

Table 3.1: BMS test reference signals.

Battery Power Reference [p.u]	Time of Implementation [s]
1.0	100
1.5	1000
-1	4000

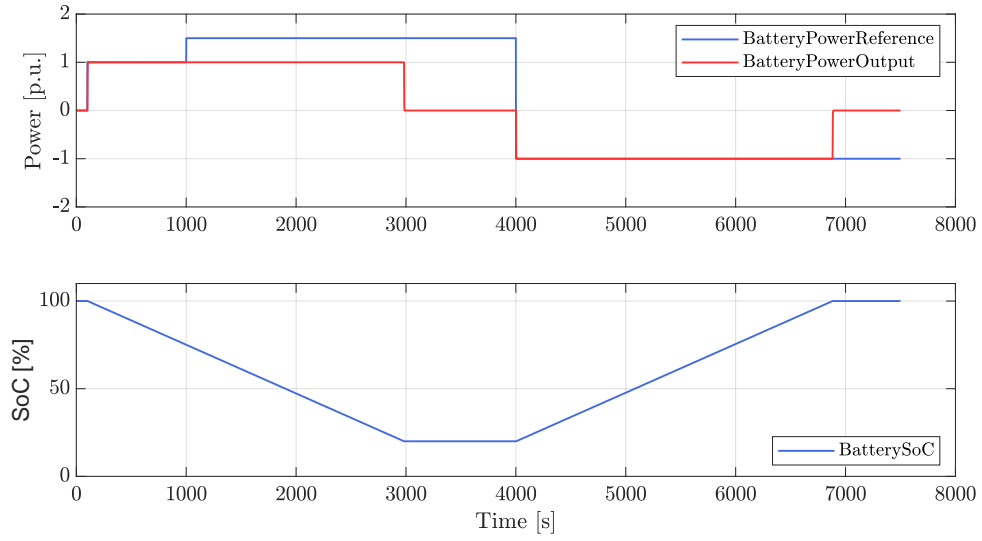


Figure 3.7: Verification of BMS model for power output and SoC.

It is verified that the BESS is functioning as intended i.e.

- Discharging with positive reference and charging with negative reference.
- SoC varies within 20% to 100%.
- The output power of the BESS is limited to 1 p.u. even if the reference exceeds it at 1000 s, as the BMS limits it to the maximum rating.

BESS Current Controller

The current controller for the BESS has an outer PQ control loop and an inner current control loop as shown in Figure 3.5. These loops are modelled as DSL models. The outer PQ control loop receives its reference signal from the BMS and power measurement signal from the BESS. Based on the PI-controller reference current signal i_d^* and $i_q^* = 0$ are generated. These reference current signals are used in the inner current loop to provide the required voltage references v_d^* and v_q^* to the static generator modelled as BESS to generate the active power as per the HPP controller reference.

Figure 3.8 shows the PI controllers' combined performance in both loops before and after tuning.

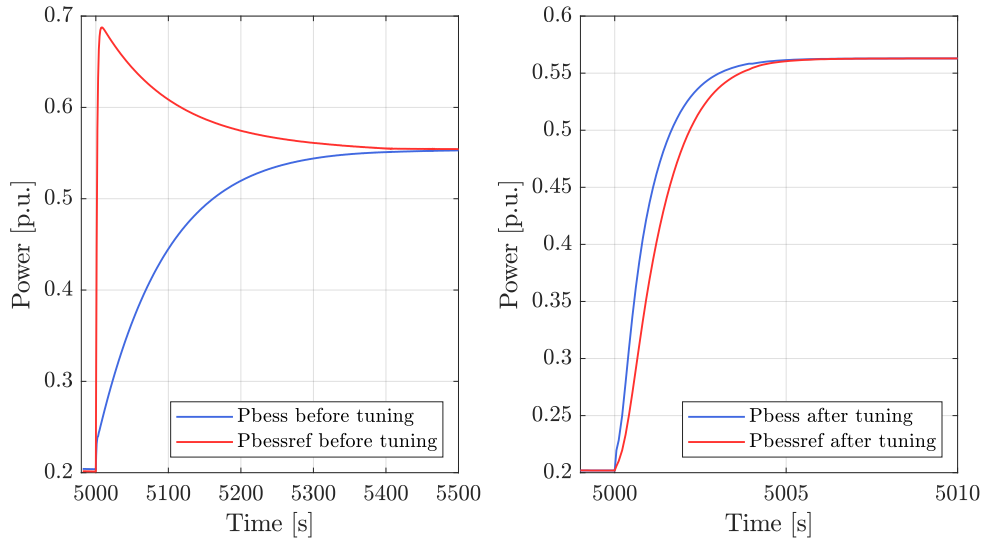


Figure 3.8: Performance of BESS current controller before and after tuning.

First the tuning for the PI controller in the inner current loop is performed using the MATLAB siso-tool and the system is represented in Figure 3.9.

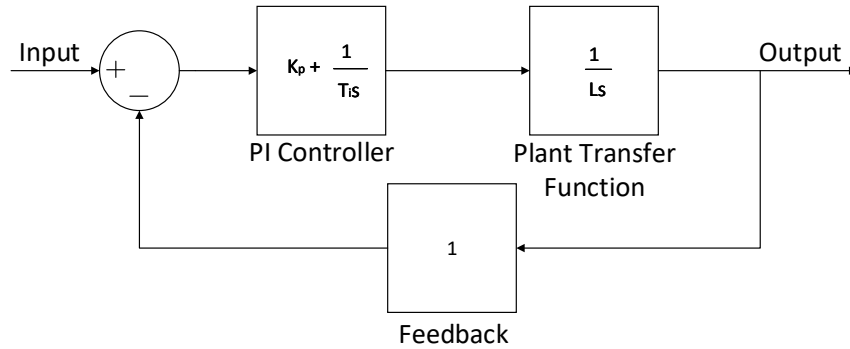


Figure 3.9: SISO representation of the inner current loop for tuning.

The static generator used to model the BESS has an internal series reactor with a short circuit impedance of 10%. This provided the value of $L = 0.32 \cdot 10^{-3} p.u$ for the plant transfer function at 50 Hz system frequency. Then the outer PQ loop was tuned to be ten times slower as per the control theory principles. The parameter values are provided in Section 3.3.4.

3.3.4 Control Loop Parameters

The relevant K_p and T_i parameters for all the PI controllers present in the modelled control loops are stated in Table 3.2. The secondary frequency PI controller in the HPP controller model, has been tuned to be slower than the PQ control loop in the BESS controller.

Table 3.2: Control loop parameter values.

Loop	Controller	Parameter	Value
PQ	BESS	Kp	0.09
		Ti	0.03
Current	BESS	Kp	0.997
		Ti	0.0033
Secondary frequency	HPP	Kp	0.1
		Ti	0.06

3.4 Chapter Summary

This chapter explains the modelling of the investigated HPP. The overall description of the system is presented providing the structure and the connection of the system. Then, a brief description of the elements included is given. Following that, the controllers which are the major factor determining the plant's behavior are explained with the diagrams implemented as DSL models provided. The actual PowerFactory schematics can be found in Appendix C. The various codes developed to respond to the grid codes requirements related to the frequency control modes and also the battery responses for AS are stated.

4 Study Cases

In this chapter, the test cases are described providing the relevant results obtained from the implemented analysis. Test case 1 is executed to provide a match between the forecasted power committed to the grid and the actual produced power from RES, using the BESS. Furthermore, different battery sizes are tested to observe the battery capabilities based on their capacity. The next scenario explored in test case 2 is the case where there is a frequency deviation and the battery responds to provide primary frequency support through frequency AS. Thereafter, test case 3 deals with a negative spot price as a market scenario. An economic analysis is made for this case to calculate the profit that can be obtained in this situation. The following Table 4.1 summarises the tests executed in each case and includes the settings required to be preset, in HPP controller (*Enable Key*) and in BESS controller (*Activation Key*).

Table 4.1: Cases summary and settings in the controllers.

Case Title	Tests	Enable Key	Activation Key
Case 1: Forecast Matching	Active power support for HPP	0	0
Case 2: Frequency AS	Primary frequency response, Secondary frequency response	1	0
Case 3: Effect of Spot Price	Curtailement scenario, Economic analysis	0	1

4.1 Case 1: Forecast Matching

The first test case executed verifies the operation of the plant, the battery, and the controllers developed in the model to provide the forecasted power. In this scenario a fixed predicted power from the HPP is accepted by the TSO in a bid to supply the grid. This is the power that needs to be supplied by the HPP using the BESS, in case of variations in production. Moreover, different battery sizes, based on power rating and energy capacity, are tested to observe which capacity is more suitable to complement the installed RES.

The exact data are not mentioned due to confidentiality, as real data for actual production

4. Study Cases

is used and a simple estimation of the forecasting has been provided. This estimation has a different accuracy level as compared to the actual forecast used for market participation. A system power loss of approximately 6% is considered for the analysis.

For the power mismatch calculation signal to be used as the reference to the battery, the parameters on Table 4.1 need to have the respective values.

The forecasted PV and wind power have a profile as illustrated in Figure 4.1 with blue colour while the produced power is shown with red colour. Due to the wind speed variation and changes in solar irradiation, the produced power varies from the promised power and the battery needs to complement them and fulfil the mismatch. The average variation of the total forecasted production and the actual one is approximately 3.2 MW, 4.8% of the total RES capacity. The maximum positive deviation is approximately 9.18 MW (24% deviation from production) and the minimum positive deviation is approximately 1 MW (2%). The maximum negative deviation is -1.7 MW ($\approx 2.5\%$).

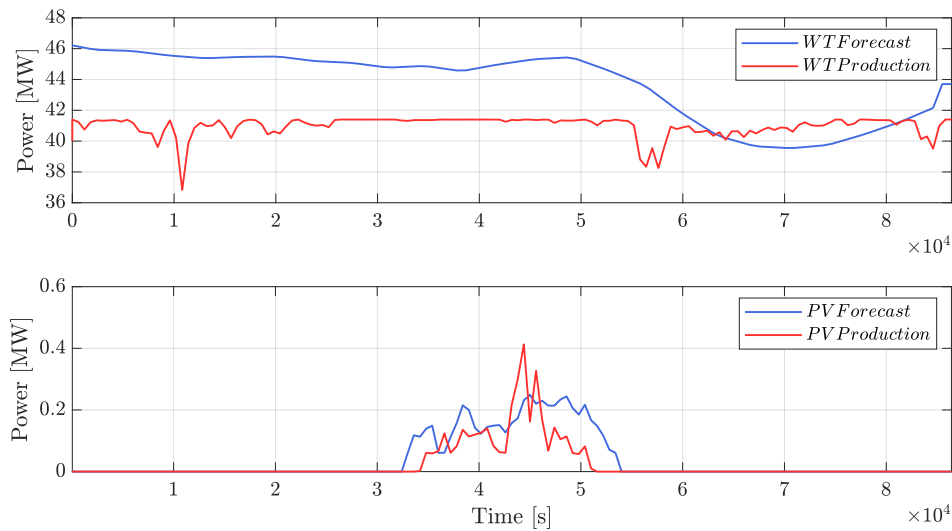


Figure 4.1: RES production data and estimated forecast.

The first scenario that is implemented is with a BESS with a converter rating of 5 MW and SoC at 100%. In this case, it is observed that this converter capacity is not high enough to support 100% production mismatch for the whole day, so a higher converter size is implemented.

A BESS with 10 MW converter rating and SoC at 50% is tested thereafter. The obtained response is illustrated in Figure 4.2 where the battery can not provide the exact mismatch signal due to its SoC. After approximately five and a half hours the battery stops following the power mismatch signal for almost 11 hours until it can charge. Specifically, when the SoC drops to 20% the BESS stops providing the missing power. If the battery is

4. Study Cases

not fully charged initially, it does not have as much stored power as required to provide and cover the mismatch. When it gets a signal to store energy it can charge and continue responding based on the need and the BESS SoC condition as the BESS provides power only above 20% SoC.

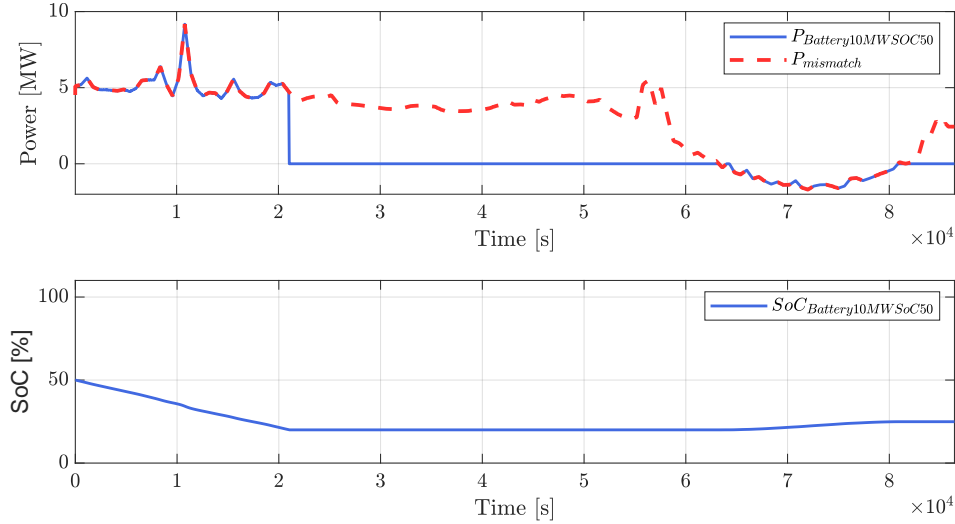


Figure 4.2: Power mismatch signal and battery power for 10 MW and initial SoC at 50%.

The next test is conducted with the SoC initially at 100%. Figure 4.3 shows the obtained results from this test case. The battery is able to fully respond and complement the power mismatch of forecasted and actual RES production for the whole day as the power output follows the mismatched signal. The fully charged battery capacity allows discharging of the battery for the whole required time duration as shown in the second plot.

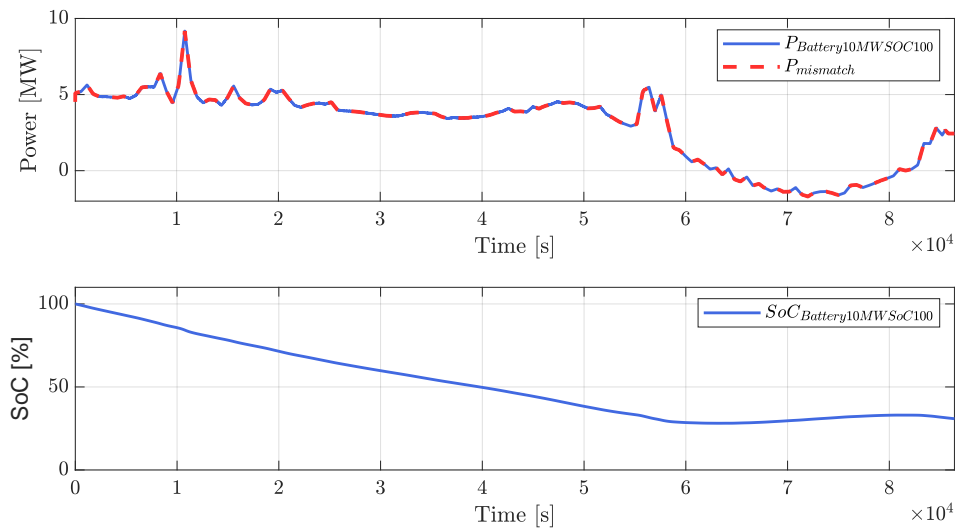


Figure 4.3: Power mismatch signal and battery power.

4. Study Cases

The formulas used for performance calculations are given by Equations 4.1 and 4.2.

$$\text{Duration Support Capability}[\%] = \frac{\text{Duration of Support}}{\text{Total Duration Considered}} \cdot 100 \quad (4.1)$$

$$\text{Power Support Efficiency}[\%] = \frac{\text{Power Supported by BESS}}{\text{Total Power Deficit}} \cdot 100 \quad (4.2)$$

The duration support capability defines how long the BESS can support the expected plant operation in percentage of the total operation time and the power support efficiency indicates the percentage of power that can be provided with respect to the mismatched power that should have been provided. Table 4.2 collects the results for duration support capability and power efficiency from the tests implemented using different battery sizes and various initial SoC conditions. In Appendix F the relevant graphs can be found for the various tests.

Table 4.2: BESS performance based on sizes for average mismatch of 3.2 MW and total deficit of 7.5 %.

Battery Converter Rating [MW]	Battery capacity [MWh]	Initial SoC [%]	Duration Support Capability [%]	Power Support Efficiency [%]
5	100	100	100	97.4
10	100	100	100	100
		80	76.4	82.2
		50	44.3	44.2
20	120	80	100	100
		50	50.1	51.8
	100	100	100	100
		80	76.4	82.2
	50	100	54.4	56.8
	20	100	38.9	29.2

The success criteria are defined as the provision of 100% power support for 100% duration for this test case as the market economics are not considered.

4.1.1 Conclusions of Case 1

From the implementation of this case, it can be concluded that despite inaccuracy in the forecasted data, the battery can cover the lack of power based on its energy and power ratings as shown in Table 4.2. The BESS responds accurately to the input signals it receives and charges or discharges accordingly.

Furthermore, from the various test results, it can be concluded that the battery with a converter rating of 10 MW and energy capacity of 100 MWh can be sufficient to fulfil the plant's power deficit of approximately 7.5 % based on production since it has duration and power support of 100% when it provides for the whole day at 100% SoC. In addition,

it can provide 76.4% and 82.2% respectively at 80% SoC. This conclusion can differ when it is decided to provide only for the limited, economically optimised time and not for the whole day, as the priority between the duration capability and the power efficiency will vary. A short-time implementation can be carried out with a smaller battery. Similarly, a smaller BESS can be used to smoothen the response of fluctuating PV production due to a fast-moving cloud.

4.2 Case 2: Frequency Ancillary Services

In this scenario, primary and secondary frequency support through frequency AS is provided to the grid through the BESS as a response to a frequency deviation due to a 25% increase in the external load at 50 s. This case requires some parameter initialisations in the controllers as stated in Table 4.1. The performance of BESS from the previous test case with a converter rating of 10 MW is compared to a 1 MW converter for primary response and 20 MW for a secondary response. The time based criteria for FSM and LFSM are stated in Table 4.3.

Table 4.3: Activation time criteria for FSM and LFSM active power response for Power Park Module (PPM) for CE and Nordic area [36], [37].

Criteria	Time
Initial delay for FSM	$\leq 500ms$
Initial delay for LFSM	$\leq 2s$
100% Response Activation	30s

The primary response provided by the BESS after the event, at 50 s, is shown in Figure 4.4. The test is executed with different droop settings for the LFSM-U and various converter ratings to observe the system behaviour. The legend in the figure states the droops for the corresponding modes and the BESS converter rating in *MW*. As the load increases the frequency drops to a minimum value. Immediately due to frequency deviation the BESS gets activated and discharges to provide primary frequency response. This response limits the frequency drop at the nadir by providing constant active power support. After 30 s of initiation of the primary response, the secondary response is observed to be activated which will be further analysed at a later point.

4. Study Cases

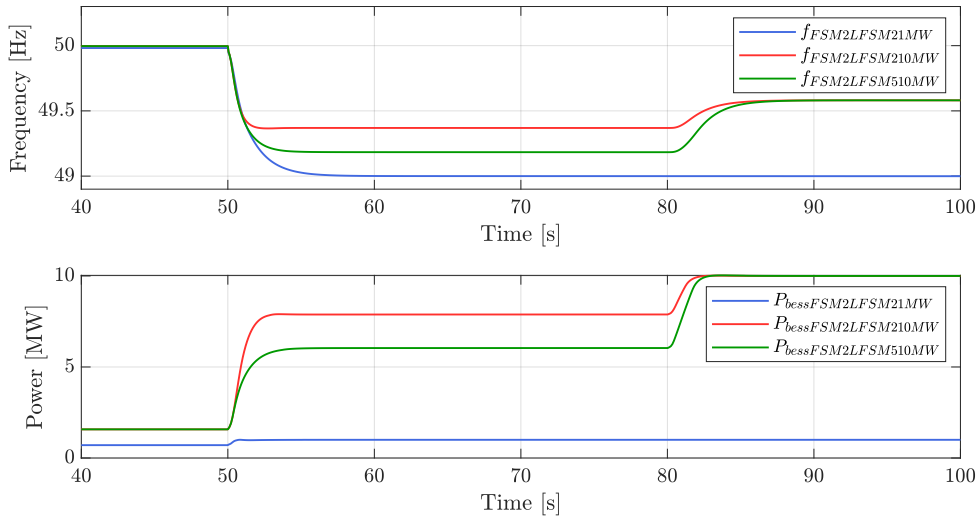


Figure 4.4: Frequency excursion and BESS power profile as primary response with different droop settings and convert ratings.

The obtained results to determine the FCR performance at FSM mode are stated in Table 4.4.

Table 4.4: FCR performance at FSM droop for different BESS converter ratings.

BEES Converter Rating [MW]	FSM Droop [%]	Response Time [ms]	Power Based on FSM Droop at 49.8 Hz [MW]	Measured Power for FSM Response [MW]	Error [%]
1	2	300	0.2	0.17	-15
10	2	300	2	2.23	+11.5

Based on [23] the tolerance limits of the active power delivered as a response are +15% or -5% and it is considered beneficial to over-deliver the promised power than under-deliver it. From the test, it is observed that the BESS converter rating of 10 MW is delivering within the performance band however 1 MW can not supply within these limits as the error reaches -15%. However, both have a fast response time of 300 ms.

The power based on droop should have a linear behaviour. However, from these results, it is observed that there is non-linearity between the power based on droops and the actual value provided. It is derived that the dynamics of the system involving a number of controllers leads to this behaviour.

Table 4.5 states the LFSM-U response characteristics.

4. Study Cases

Table 4.5: Frequency nadir based on LFSM droop and BESS converter ratings.

BESS Converter Rating [MW]	LFSM Droop [%]	Nadir [Hz]	Response Time [s]	Power Based on LFSM Droop at Nadir [MW]	Measured Power for LFSM Response [MW]
1	2	49	8.22	1	1
10	5	49.19	4.22	4.5	6
10	2	49.37	2.22	6.3	7.8

From the table, it is observed that there is a correlation between BESS converter rating and the nadir. The higher converter rating delivered higher power leading to a higher nadir. An effect of droop is also observed when a comparison of the same converter rating with a different LFSM droop is conducted. Lower LFSM droop enables the provision of higher active power, thus preventing the frequency from falling further. The response time of the BESS in this case is defined as the time taken to reach the nadir and it is very low with 8.22 s being the maximum required time. These results conclude that a smaller droop value for a higher converter rating provided better frequency stabilisation. Moreover, due to a lack of mechanical components, the BESS responds faster within the full activation time limit of 30 s.

Moving on to the analysis of the secondary response FRR, Figure 4.5 presents the continued response of the 10 MW BESS converter at 80 s to the persisting frequency deviation.

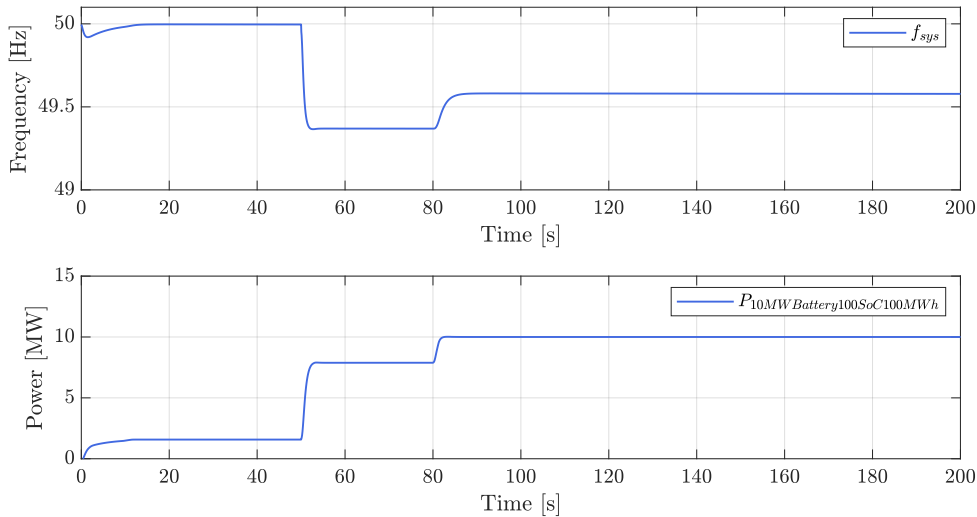


Figure 4.5: System frequency excursion and FRR response of 10 MW BESS converter.

Due to the limitation of the converter size, it is seen that the power delivered is restricted at 10 MW, which causes the frequency to stabilise at a value lower than the nominal

4. Study Cases

frequency of 50 Hz. Based on the obtained results, a decision is made to further evaluate the scenario with a higher converter rating of 20 MW. When the 20 MW of battery is used the response is as follows in Figure 4.6.

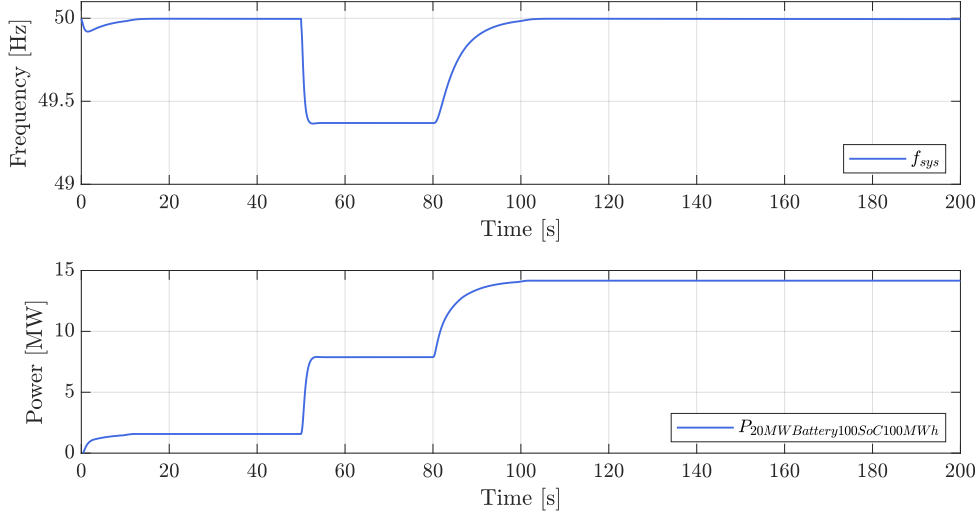


Figure 4.6: System frequency excursion and FRR response of 20 MW BESS converter.

Here, it is observed that the frequency reaches its nominal value after the load event occurring at 50 s within 20 s. This response time is faster than the required response time of 2 mins, for aFRR, as stated in Section 2.4. A summary of the comparison of the two results is presented in Table 4.6.

Table 4.6: Secondary frequency response of the HPP based on BESS converter ratings.

Battery Converter Rating [MW]	Secondary Response Delivered [MW]	Steady State Frequency [Hz]	Steady State Error [%]
10	10	49.58	0.84
20	14.2	50	0

From the above scenario the 20 MW of BESS is further analysed for the duration capability as a FRR. Different BESS energy capacities have been compared i.e. 10 MWh, 20 MWh, and 100 MWh and the responses are observed in Figure 4.7. The duration of the response changes according to the energy rating and the BESS provides active power support for a longer duration in case of the higher energy rating. The evaluated duration is until 4000 s to consider the 1 hr bidding slots of the service.

4. Study Cases

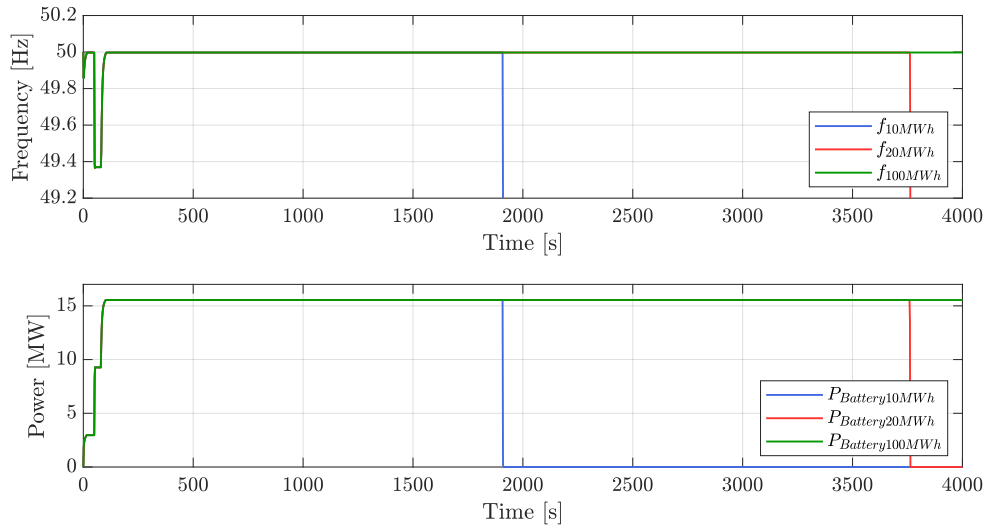


Figure 4.7: Frequency excursion and power of 20 MW battery, with 10 MWh, 20 MWh and 100 MWh energy ratings.

It is concluded that 20 MW BESS with 20 MWh rating can provide the required power support for maintaining the nominal system frequency at 50 Hz for 1 hr after a 25 % load increase event in this particular scenario.

Til now only up-regulation cases for lower frequency have been described. However, for frequency down-regulation a similar behavior is observed, when the load is decreased as shown in Figure 4.8 and no further analysis is done for this scenario.

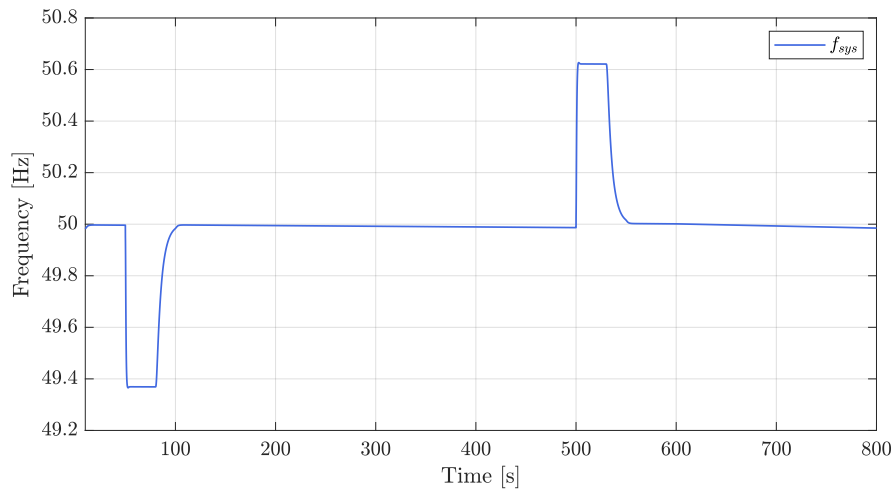


Figure 4.8: System frequency excursion for under-frequency and over-frequency events with a support from a 20 MW BESS providing FCR and FRR response.

4.2.1 Conclusions of Case 2

When a frequency event occurs in the system it can be concluded that the plant's controllers have the ability to detect this disturbance and the BESS can respond to provide frequency support to the grid. This is accomplished through the primary and secondary frequency responses fulfilling the relevant grid codes related to response time, power capacity and support duration. From the various BESS ratings that are tested the 20 MW converter with 20 MWh proves sufficient to supply the required power reserve for the tested scenario of 25 % load change. The primary performance is considered only until 30 s as after that, the secondary reserve with a higher power requirement is activated. So it is assumed that primary support by itself can be sufficiently handled for that period of time.

4.3 Case 3: Effect of Spot Price

Case 3 deals with the scenario of having over-frequency events in the system, either in a period of high production or a decrease in load leading to negative spot price. The goal is to curtail the plant's generation units and charge the BESS from the grid to aid in stabilising the system frequency. An economic analysis is made to estimate the earnings considering the curtail and down-regulation services. For this test case, the values of the controllers' keys are listed in Table 4.1.

As stated recently by Energinet, there is a need for more RES plants to be able to switch off when there is excess power in the system leading to high frequency and negative spot price. Down-regulations are necessary in these situations, however, on some occasions, this is not enough and curtailing production is required. These grid support actions increase the plant owner's profit. As an example, 7 April 2024, the downward regulation capacity went up to 99 MWh and the highest profit was 995 €/MWh, according to Energinet for a plant participating in the power market. [40], [41]

Similarly, 14 April 2024 showed negative spot prices and this data obtained from [38] is chosen for the test case which is illustrated in Figure 4.9. In this test, a higher system frequency is detected and the corresponding negative spot price is considered. On these occasions, different actions can be executed such as charging the BESS, curtailing the RES to some extent or completely, or a combination of both down-regulation and curtailment depending on the severity of the disturbance.

4. Study Cases

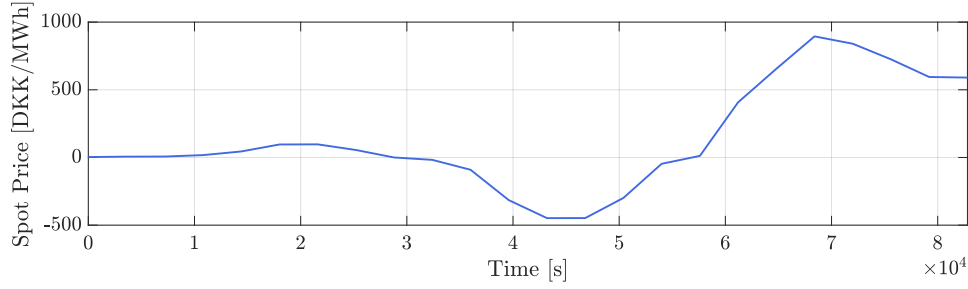


Figure 4.9: Spot price profile for 14 April 2024.

All aforementioned measures are simulated in this test case and the respective RES production profiles are illustrated in Figure 4.10. At 33 000 s, at around 9 am in Denmark, a negative spot price is detected and a rise in frequency is observed. The WTs are curtailed in multiple scenarios to observe the impact it will have on the system frequency. They can stay connected and continue their normal operation, as illustrated in the figure with blue colour. Otherwise, some WTs can be switched off in this case, either one-third (red colour) or two-thirds (green colour), or switched off entirely (purple colour). The PV park production is indicated as zero (yellow colour) since their production time corresponds to the time duration of negative spot price causing them to be switched off intentionally.

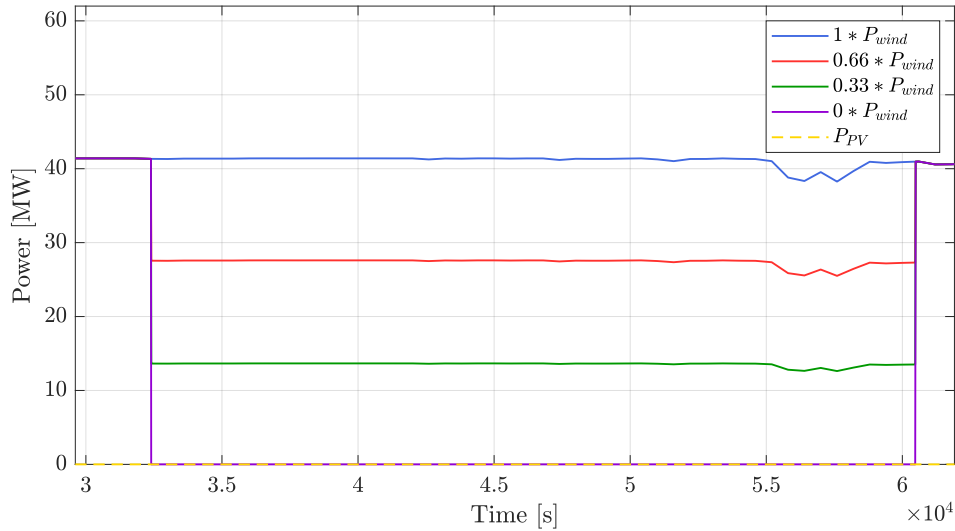


Figure 4.10: RES production profiles based on different curtailment scenarios.

The whole event of negative spot price lasts for 6 hrs and to observe the effect of BESS on this profile a converter rating of 1 MW is chosen with 4 MWh energy rating for initial analysis. In some scenarios BESS charges power from the grid as a down-regulation service and absorbs a constant excess power of 1 MW. The effect of these support combinations on the frequency during the curtailing period is shown in Figure 4.11.

4. Study Cases

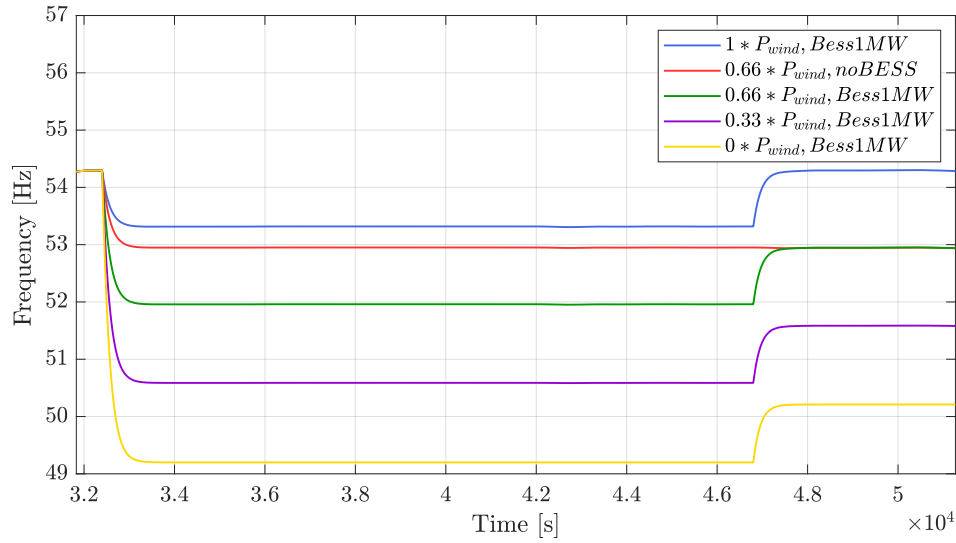


Figure 4.11: System frequency during different tested scenarios.

It is visible that the frequency is high in the initial presented instant. The frequency range is extreme due to the limitations of the simulated model. When the BESS is set to absorb 1 MW the frequency drops at a value above 53 Hz and when it is fully charged the frequency rises again. As this down-regulation capacity is not sufficient to return the frequency to its normal value, it requires production downsizing. By turning off 33% of the wind farm without charging the BESS, the frequency drops to approximately 53 Hz and remains there constantly. Alternatively, both BESS is charged and wind curtailment is implemented at various extents since a complete shutdown of the generation unit results in an under-frequency event for this particular simulation. Therefore scenarios with switching off 33% and 67% of the WTs are examined. The moment the BESS is not able to charge anymore, after 46 000 s, the frequency increases again since the effect of the BESS on frequency support terminates.

Based on Figure 4.11, the following Table 4.7, collects all the tested frequency support combinations for easier reference in the following analysis.

Table 4.7: Tests executed for system frequency support.

Support Case	Active BESS	Curtailed WTs	Curtailed PV
No.1	✓	0%	100%
No.2	X	33%	100%
No.3	✓	33%	100%
No.4	✓	67%	100%
No.5	✓	100%	100%

Additionally, an economic analysis is followed to compute the revenue when the market options are examined. The BESS of 4 MWh is replaced with a 10 MWh for the economic

4. Study Cases

analysis as a full frequency support case is preferable. The charging of the BESS from the grid is considered a down-regulation service, therefore aFRR down-regulation capacity price from the market is taken into account. The prices are found from Energinet's online data in [41].

The BESS can provide support of 1 MW from 9 o'clock to 3 o'clock afternoon. Based on the aFRR price data, the hourly revenue is calculated in Table 4.9 for this specific duration.

Table 4.8: Revenue obtained by charging the 1 MW BESS.

Hour	aFRR Price [DKK/MWh]	Revenue [DKK]
9 am	895.236	895.236
10 am	1044.442	1044.442
11 am	932.5375	932.5375
12 pm	1044.442	1044.442
13 pm	932.5375	932.5375
14 pm	1044.442	1044.44
15 pm	932.5375	932.5375
	Total revenue	6826.2

The profit that can be obtained by charging the BESS for this time slot is estimated to be approximately 6826.2 DKK/MW.

Moreover, based on each test scenario losses can be prevented by curtailment of the RES. The values are presented in Table 4.9 and 4.10 for 100% curtailment of power from WTs and PV respectively.

Table 4.9: Losses prevented by curtailing the WT production by 100%.

Hour	Spot Price [DKK/MWh]	WT Curtailment [MWh]	Loss [DKK]
9 am	-17.68	41.39	-731.77
10 am	-90.8	41.39	-3758.2
11 am	-315	41.4	-13041
12 pm	-448	41.39	-18543
13 pm	-447.7	41.39	-18543
14 pm	-298.8	41.4	-12370
15 pm	-46.6	41.39	-1928.8
		Total loss prevented	68916

4. Study Cases

Table 4.10: Losses prevented by curtailing the PV production by 100%.

Hour	Spot Price [DKK/MWh]	PV Curtailment [MWh]	Loss [DKK]
9 am	-17.68	15	-265.2
10 am	-90.8	15	-1362
11 am	-315	15	-4725
12 pm	-448	15	-6720
13 pm	-447.7	15	-6715.5
14 pm	-298.8	15	-4482
15 pm	-46.6	14.9	-694.3
		Total loss prevented	24964

The overall losses, savings and profits are stated in the Table 4.11. The WTs revenue are negative as they indicate the losses that need to be paid based on the scenarios. The PV revenue indicates the savings because of 100% curtailment, while the BESS revenue shows the profit from charging 1 MW battery. The total revenue takes into account only the profit and the losses.

Table 4.11: Net revenue that is generated by charging the BESS 1 MW on the relevant cases and curtailing the RES.

Support Case	No 1	No 2	No 3	No 4	No 5
WTs Revenue [DKK]	-68916	-46174	-46174	-22742	0
PV Revenue [DKK]	24964	24964	24964	24964	24964
BESS Revenue [DKK]	6826.2	0	6826.2	6826.2	6826.2
Total Revenue [DKK]	-62090	-46174	-39348	-15916	6826.2

From the above results, it can be concluded that curtailment is essential to avoid paying for the negative spot price whenever there is production from the HPP. In addition, revenue can be generated through BESS based on the capacity if grid support services are provided.

To generate additional revenue stream the HPP can participate in the frequency AS market, as a whole unit, to provide support for down-regulation and earn profit. In Table 4.12 the revenue generation for different reserve capacities as a percentage of the total RES capacity is stated for the particular price.

4. Study Cases

Table 4.12: HPP revenue through aFRR participation based on RES contribution.

RES Contribution [%]	aFRR Support [MWh]	Revenue [DKK]
15	10	68262
30	20	136524
45	30	204786
60	40	273048
75	50	341310
90	60	409572

From the above results, it is observed that participating in the market will contribute to reducing the LCoE while stabilising the grid.

4.3.1 Conclusions of Case 3

In the initial scenario of Case 3, due to a high negative spot price, only providing system services through the BESS still leads to revenue losses without significantly improving the system frequency. However, curtailing leads to preventing losses and improves the system frequency to a greater extent. When this curtailment is provided as a system service in the form of aFRR, it leads to a higher income even though the effect on the system frequency remains the same. Hence, careful market analysis should always be considered as a part of HPP operating conditions to support the grid while generating revenue.

It can also be argued that it is better to absorb minimum power to maintain the DC link voltages without operating the WTs and PV than to generate at a negative spot price for the IBRs. This would not only benefit the plant owners by preventing losses but also facilitate the TSOs to stabilise the grid frequency.

4.4 Chapter Summary

This chapter includes different test cases implemented to observe and further understand the operation of the modelled HPP under specific conditions. In the first case, the BESS operates to provide the mismatch between the actual production and the forecasted production. Different BESS capacities, converter ratings and initial SoC are tested to observe the support capabilities of the BESS under different sizes. The BESS converter rating of 10 MW with a high energy rating of 100 MWh proved sufficient for the particular system. The second test case simulates a frequency event with a change in load so frequency AS can be provided to the grid. It is concluded that the HPP with a 20 MW BESS converter with 20 MWh energy rating can provide primary and secondary frequency response through AS by complying with the grid codes. From these test cases, it is observed that the BESS can support the grid by either improving the overall performance of the plant or through system services. The third test case implements an over-frequency

4. Study Cases

event, with a negative spot price in the market, to analyse the economics of curtailment and aFRR provision. It is shown that the BESS can absorb from the grid whenever a negative spot price is detected gaining profit and when the RES are curtailed the system frequency becomes more stable. It is concluded based on economic calculations that curtailment prevents losses and if participation in the market is considered profit can be earned.

5 Discussion

As the modelling part of this project is an important aspect of the successful operation of the scenarios, it is seen that the BESS modelling affects its behaviour. For example, under the same event, the response differs based on the battery model used in Power-Factory. With a static generator (constant power mode and generator oriented) the nadir goes lower than when using a controllable load. Additionally, with the controllable load, the SoC gets lower values while with the generator it reaches a higher percent of SoC increasing the number of charging cycles of the battery. With a controllable load, the response was faster than compared to the generator. Furthermore, the PLL does not show oscillations with the static generator while with controllable loads the signal has more oscillations as the static generator has local controllers which introduce a delay and make it respond slower. Thus, this signifies the use of proper models for analysing the behaviour in focus.

Real data was used for the various scenarios and data analysis was required. Because of its vast volume and the need to extract and validate the data value and parameters, the process was time demanding.

A simple estimation of the forecasting has been utilised in the project which has a lower accuracy level as compared to the actual forecast used for market participation to maintain confidentiality. This emphasises that when a better forecast is used, a more beneficial economic prognosis can be made.

In this project, the external grid modelled is a weak grid and the system frequency stability depends mostly on the HPP support capability. This can assume that the system is islanded where no external systems can support the grid. In realistic situations, the Danish grid is a strong grid, so the impact the modelled plant has on the system is much smaller than the results obtained. Therefore, it is not expected that one plant will fully restore the system frequency as other reserves will also provide support services simultaneously. Moreover, when the BESS cannot further provide power when required, it necessitates procuring the power mismatch from other market participants. This way a penalty from the TSO company is avoided when the accepted bidded power is not provided.

In addition to the requirements that are fulfilled, the success criteria are also dependent

on multiple other factors which have not been considered in these cases like reactive power compensation, fault tolerance capabilities, battery lifetime considerations, and degradation.

Splitting the battery capacity is a feature investigated by companies to find the optimised BESS operation. In this case, the whole BESS capacity is used for each service that is provided. There is the possibility to split the capacity into different parts so reserve is kept to provide for other services. Likewise, when the BESS size is high enough it gives more available capacity for other services. It is worth mentioning that only some battery sizes are considered for each test case however optimisation can be done based on the services the plant owner wants to provide and its extent.

From an economic perspective, the grid codes need to be defined clearly in a way which should prevent the participating entities from causing the problem and benefiting from it. For instance, if the loss from the spot price is low, a dispatchable generating unit can keep producing while a co-located storage unit keeps earning revenue at the cost of the system's stability.

6 Conclusion

A higher percentage of IBRs in the energy mix leads to a dynamic grid situation where the prediction accuracy decreases significantly as compared to the traditional system with synchronous generators as majority. This causes system frequency instabilities which can be tackled by active power regulation. HPPs aid in better use of natural resources like land as well as provide a higher utilisation factor than individual units. At times of excess power, a lot of unnecessary curtailment is required which can otherwise be stored. The benefits of energy storage like BESS, as a component of an HPP and the significance of active power regulation for system stability are validated in this project. Successful model validations were conducted before initiating test cases for the developed controllers. The main objectives defined in this project have been successfully executed as described below.

Forecast matching is crucial as it decides the bidding power in the market that the plant should be able to deliver. This importance is analysed in the project and accomplished with the BESS covering the mismatch between the actual production and the estimated forecast.

The project emphasises the need for frequency support services for a system with low inertia, where BESS can aid in this balance. The second test case confirms when a frequency event occurs in the system, the BESS can provide active power regulation through primary and secondary frequency responses adhering to grid compliance. Additionally, the significance of battery sizing is also highlighted.

It is inferred from a higher frequency event that charging the BESS is not always sufficient to return the frequency to its nominal value so curtailment of the RES becomes a necessity. The aforementioned process combined with the occurrence of negative spot prices leads to losing, saving or generating revenue as per the energy market participation. This economic analysis can consequently lead to reducing the LCoE while stabilising the grid.

7 Future Work

The upcoming flexible power system with a majority share of renewables expanding at a rapid rate is facing contemporary challenges. The uncertainty of generation is leading to the introduction of newer regulations as well as market opportunities. This project has considered some of the aspects related to the frequency stability of a power system, however, there are many other aspects which can be studied by the expansion of this project.

In addition to the developed test cases and the provision of the already examined services, more options can be examined to analyse the full potential of the plant. For example, arbitrage can be examined from spot price graphs, absorbing from the grid when power is cheap and then selling to the grid later when the price increases.

If cases one and two are combined it is possible to make an economic analysis to find the most profitable way to operate the battery. For instance, it might be beneficial to have the battery on 80% SoC and utilise the other 20% from support of AS. Likewise, it might be more beneficial to have 100% available capacity for the forecast balance instead of buying the rest of the power from the market. Similar possible scenarios can be developed to examine all options.

The sudden variations or flickers in PV production due to a fast-moving cloud give rise to higher ramp rates. This maximum speed of change in active power needs to be limited according to the grid codes. To achieve this additional control functions need to be added to the already existing controllers for both upward and downward regulation to a maximum value of 20% of installed capacity per minute, without exceeding 60 MW/min and minimum 1% [15]. This can be achieved either by limiting the ramp rate of the PV or with the aid of BESS.

Further studies on current grid codes can be executed to create consistency specifically for HPPs and batteries. More clarifications can be made relevant to the AS provided by batteries along with sizing guidelines.

Optimisation problems with relevant boundary conditions can provide further insight into battery sizing. A detailed analysis of battery sizing can be elaborated taking into consideration the economic aspects with particular ways of operating the batteries. Degradation and battery life can be included in these analyses and a suitable decision on the

BESS capacity can be made.

Moreover, in this project, AC bus is modelled to connect the BESS with the PV. However, coupling them can be done with a DC-DC bus decreasing the number of inverters required. The limitations, as well as advantages of this configuration, can be elaborated by examining both the allowed grid services and operations along with their economic costs.

This project is limited to GFM converters whereas, there is the possibility to combine both GFM and GFL converters in power systems to enhance the stability and efficiency of the system. With the GFM the frequency and voltage references can be created for black start capability. This approach requires more control algorithms to examine and manage the interactions of the two converter modes. [42]

Furthermore, the analysis of voltage stability and reactive power compensation can be included in addition to frequency and active power regulation in order to examine all the aspects of system stability.

Bibliography

- [1] *Net Zero by 2050 – Analysis* - IEA. [Online]. Available: <https://www.iea.org/reports/net-zero-by-2050> (visited on 04/02/2024).
- [2] WindEurope, *Hybrid renewable power plants make a good business case but need clearer legislation to become more widespread* | WindEurope. [Online]. Available: <https://windeurope.org/newsroom/news/hybrid-renewable-power-plants-make-a-good-business-case/> (visited on 02/26/2024).
- [3] H. Habbou, J. P. M. Leon, and K. Das, "Profitability of hybrid power plants in European markets", in *Journal of Physics: Conference Series*, vol. 2507, Institute of Physics, 2023.
- [4] Energy.gov, *Wind Energy Technologies Office* | Department of Energy. [Online]. Available: <https://www.energy.gov/eere/wind/wind-energy-technologies-office> (visited on 02/26/2024).
- [5] P. Du, J. Wang, W. Yang, and T. Niu, "Multi-step ahead forecasting in electrical power system using a hybrid forecasting system", *Renewable Energy*, vol. 122, pp. 533–550, Jul. 2018.
- [6] J. S. Rounkvist, P. Enevoldsen, and G. Xydis, "High-resolution electricity spot price forecast for the danish power market", *Sustainability (Switzerland)*, vol. 12, no. 10, May 2020.
- [7] O. Lindberg, "Analysis and Forecasting of Utility-Scale Hybrid Wind and PV Power Parks", Tech. Rep., 2022. [Online]. Available: <http://urn.kb.se/resolve?urn=urn:nbn:se:uu:diva-481642>.
- [8] K. Lindgren, "Dynamic Control, Modeling and Sizing of Hybrid Power Plants", Tech. Rep., 2023.
- [9] F. Gonzalez-Longatt, J. M. Roldan-Fernandez, H. R. Chamorro, S. Arnaltes, and J. L. Rodriguez-Amenedo, "Investigation of inertia response and rate of change of frequency in low rotational inertial scenario of synchronous dominated system", *Electronics (Switzerland)*, vol. 10, no. 18, Sep. 2021.
- [10] J.R. PILLAI, "Advanced Course in Electrical Power Systems, AAU", Tech. Rep., 2023.

- [11] V. Knap, S. K. Chaudhary, D. I. Stroe, M. Swierczynski, B. I. Craciun, and R. Teodorescu, "Sizing of an energy storage system for grid inertial response and primary frequency reserve", *IEEE Transactions on Power Systems*, vol. 31, no. 5, pp. 3447–3456, Sep. 2016.
- [12] F. Teng, M. Aunedi, D. Pudjianto, and G. Strbac, "Benefits of demand-side response in providing frequency response service in the future GB power system", *Frontiers in Energy Research*, vol. 3, no. AUG, 2015.
- [13] J. Machowski, J. W. Bialek, J. Bumby, and D. J. Bumby, *Power System Dynamics - Stability and Control (2nd Edition)*, eng, 2nd ed. New York: Wiley - IEEE Press, 2008.
- [14] P. Kundur, *Power system stability and control*, eng, Second edition., O. P. Malik, Ed. New York: McGraw Hill Education, 2022.
- [15] A. D. Hansen, K. Das, P. Sørensen, P. Singh, and A. Gavrilovic, *European and indian grid codes for utility scale hybrid power plants*, Jul. 2021.
- [16] Energinet, "ANCILLARY SERVICES TO BE DELIVERED IN DENMARK - TENDER CONDITIONS", Tech. Rep., 2023. [Online]. Available: <https://en.energinet.dk/Electricity/Ancillary-Services/Tender-conditions-for-ancillary-services/> (visited on 09/20/2023).
- [17] D. Chatterjee and T. Louka, "Active Power Regulation in Hybrid Power Plants for Grid Frequency Support MSc 3rd Semester Report", Tech. Rep., 2023. [Online]. Available: <http://www.energy.aau.dk>.
- [18] Energinet, "VEJLEDNING RFG, Tilslutning af produktionsanlaeg til transmission-nettet Requirements for Generators(RfG)", Tech. Rep., 2020.
- [19] Energinet, *Electricity market*. [Online]. Available: <https://en.energinet.dk/Electricity/Electricity-market/> (visited on 02/19/2024).
- [20] "Regulation C1-Terms of balance responsibility", *Energinet*, Jan, 2011.
- [21] Energinet, "Player in the electricity market-how does it work, and who does what?", Tech. Rep. Doc. no. 16/04173.
- [22] *Price calculation | Nord Pool*. [Online]. Available: <https://www.nordpoolgroup.com/en/trading/Day-ahead-trading/Price-calculation/> (visited on 02/21/2024).
- [23] Energinet, "Prequalification of Units and aggregated portfolios", Tech. Rep. [Online]. Available: <https://en.energinet.dk/Electricity/Ancillary-Services/Prequalification-and-test/> (visited on 05/03/2024).
- [24] H. Holttinen, J. Kiviluoma, V. Nicolaos Cutululis, *et al.*, "Ancillary services: technical specifications, system needs and costs. Deliverable D 2.2", Tech. Rep., 2012.
- [25] D. V. Pombo, "Coordinated Frequency and Active Power Control of Hybrid Power Plants An Approach to Fast Frequency Response", Tech. Rep. [Online]. Available: <http://www.aau.dk>.
- [26] J. Reilly, R. Poudel, V. Krishnan, *et al.*, "Hybrid Distributed Wind and Battery Energy Storage Systems", Tech. Rep., 2022. [Online]. Available: www.nrel.gov/publications..

BIBLIOGRAPHY

- [27] Petersen, Lennart, "Proof-of-Concept on Next Generation Hybrid Power Plant Control, Aalborg Universitet", Tech. Rep., 2020.
- [28] Oliver Schmidt and Iain Staffell, ""Monetizing Energy Storage"", Tech. Rep. [Online]. Available: <https://academic.oup.com/book/55104>.
- [29] Ramboll, "ANCILLARY SERVICES FROM NEW TECHNOLOGIES", Tech. Rep., 2019. [Online]. Available: <https://ramboll.com>.
- [30] K. Dykes, J. King, N. Diorio, *et al.*, "Opportunities for Research and Development of Hybrid Power Plants", Tech. Rep., 2020. [Online]. Available: <https://www.nrel.gov/docs/fy20osti/75026.pdf>.
- [31] R. Teodorescu, M. Liserre, and P. Rodriguez, *GRID CONVERTERS FOR PHOTO-VOLTAIC AND WIND POWER SYSTEMS* (Wiley - IEEE), eng, P. Rodriguez and M. Liserre, Eds. Chichester, West Sussex: Wiley, 2011.
- [32] Vestas, *Vestas 4MW Platform—Page 18*. [Online]. Available: <https://nozebra.ipapercms.dk/Vestas/Communication/4mw-platform-brochure/?page=18>.
- [33] D. GmbH, "Technical Reference External Grid", Tech. Rep., 2022. [Online]. Available: <https://www.digsilent.de>.
- [34] *Knowledge Base PowerFactory - DIgSILENT*. [Online]. Available: <https://www.digsilent.de/en/faq-reader-powerfactory/how-is-the-external-grid-modeled-for-rms-simulation.html>.
- [35] B. Tan, J. Zhao, M. Netto, V. Krishnan, V. Terzija, and Y. Zhang, "Power system inertia estimation: Review of methods and the impacts of converter-interfaced generations", *International Journal of Electrical Power and Energy Systems*, vol. 134, Jul. 2021.
- [36] ENTSO-E, "Limited frequency sensitive mode ENTSO-E guidance document for national implementation for network codes on grid connection", Tech. Rep., 2018.
- [37] ENTSO-E, "Frequency Sensitive Mode ENTSO-E guidance document for national implementation for network codes on grid connection", Tech. Rep., 2018.
- [38] Energinet, *Energi Data Service | Datasets | Elspot Prices*. [Online]. Available: <https://www.energidataservice.dk/tso-electricity/Elspotprices> (visited on 05/02/2024).
- [39] S. H. Kim and Y. J. Shin, "Optimize the operating range for improving the cycle life of battery energy storage systems under uncertainty by managing the depth of discharge", *Journal of Energy Storage*, vol. 73, Dec. 2023.
- [40] Energinet in ENERGIWATCH, *Producenter af grøn strøm går glip af indtjening: Tudetosseset mener Energinet*. [Online]. Available: https://energiwatch.dk/Energinyt/Energiselskaber/article17087846.ece?utm_source=linkedin (visited on 05/19/2024).
- [41] *Energi Data Service | Datasets | aFRR, Activated Automatic Frequency Restoration Reserves*. [Online]. Available: <https://www.energidataservice.dk/tso-electricity/AfrrActivatedAutomatic> (visited on 05/20/2024).

BIBLIOGRAPHY

- [42] NREL Transforming Energy, *Technical Roadmap Guides Research Direction for Grid-Forming Inverters* | News | NREL. [Online]. Available: <https://www.nrel.gov/news/program/2020/technical-roadmap-guides-research-direction-grid-forming-inverters.html> (visited on 05/27/2024).

A Modelling Parameters

A.1 Substation Transformer Parameters

The following table shows the substation transformer parameters used in this project.

Table A.1: Substation transformer parameters.

Parameter	Value
Rated Power	80 MVA
Nominal Frequency	50 Hz
Rated Voltage	33/63 kV
Connection Group	$Ynd11$
Short Circuit Voltage	10%
Load Losses	241+15 %kW
No load Current	0.12%
No load Losses	22+15 %kW

A.2 Cable Line Parameters

Table A.2 indicates the values that are used for the cable line in the modelled system.

Table A.2: Cable Line 1 parameters.

Cable	R' [$\frac{\Omega}{km}$]	L' [$\frac{mH}{km}$]	C' [$\frac{\mu F}{km}$]	Length [km]	Rated Voltage [kV]	Rated Current in ground [kA]
Line 1	103.37	248.08	817.08	0.001	36	770

B Controller Block Diagrams

Figures B.1, B.2 illustrate the enlarged HPP and BESS controller respectively.

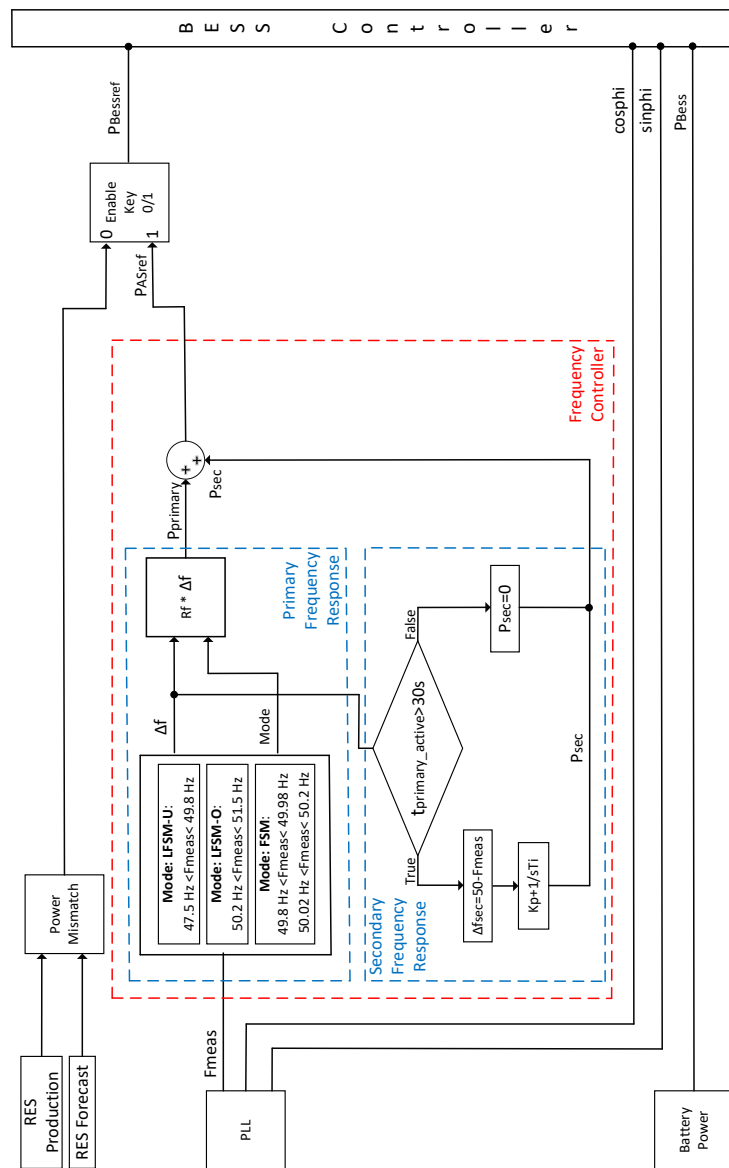


Figure B.1: Enlarged figure of HPP controller architecture.

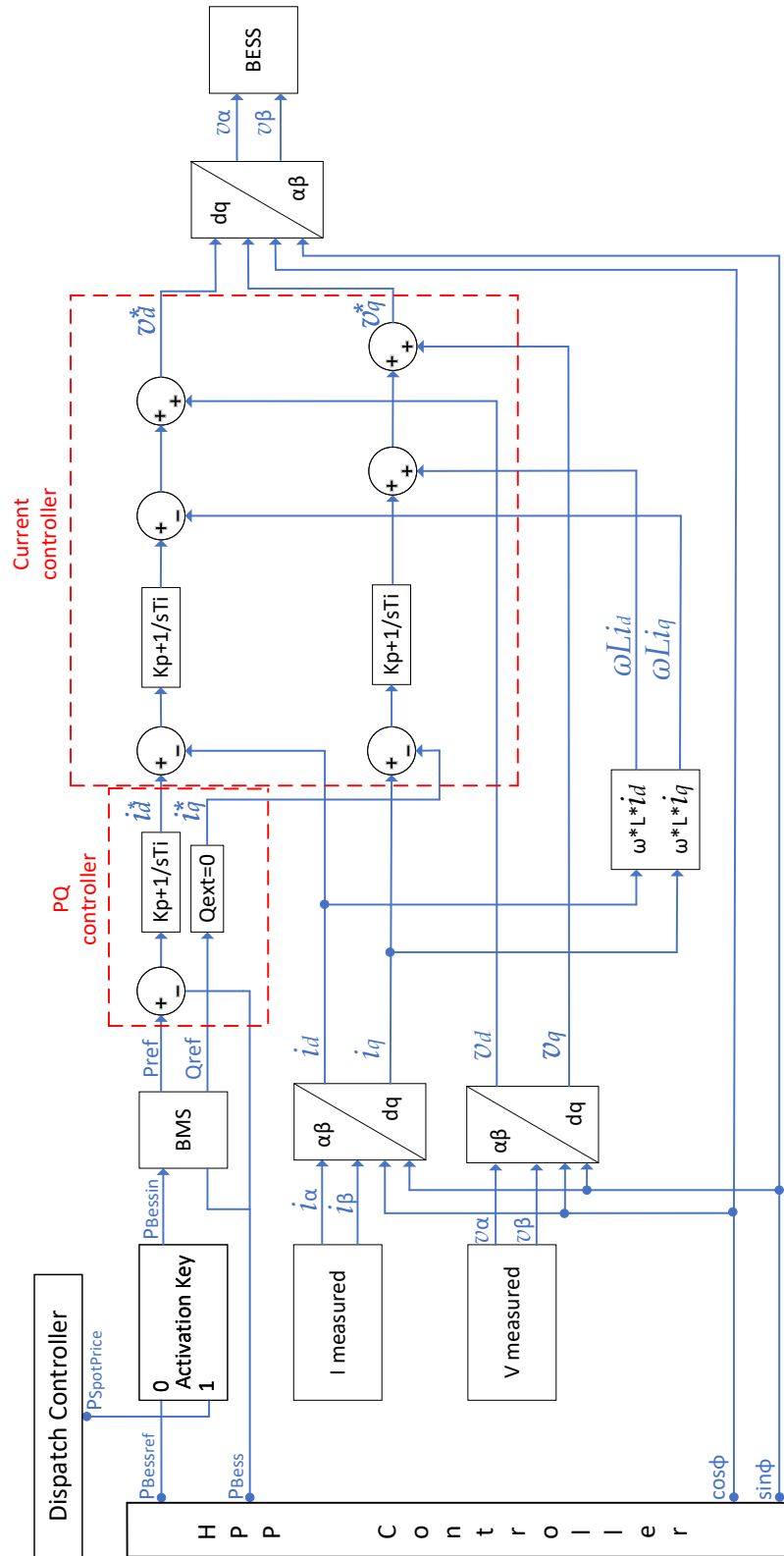


Figure B.2: Enlarged figure of BESS controller architecture.

C PowerFactory Model Diagrams

HPPcontroller:

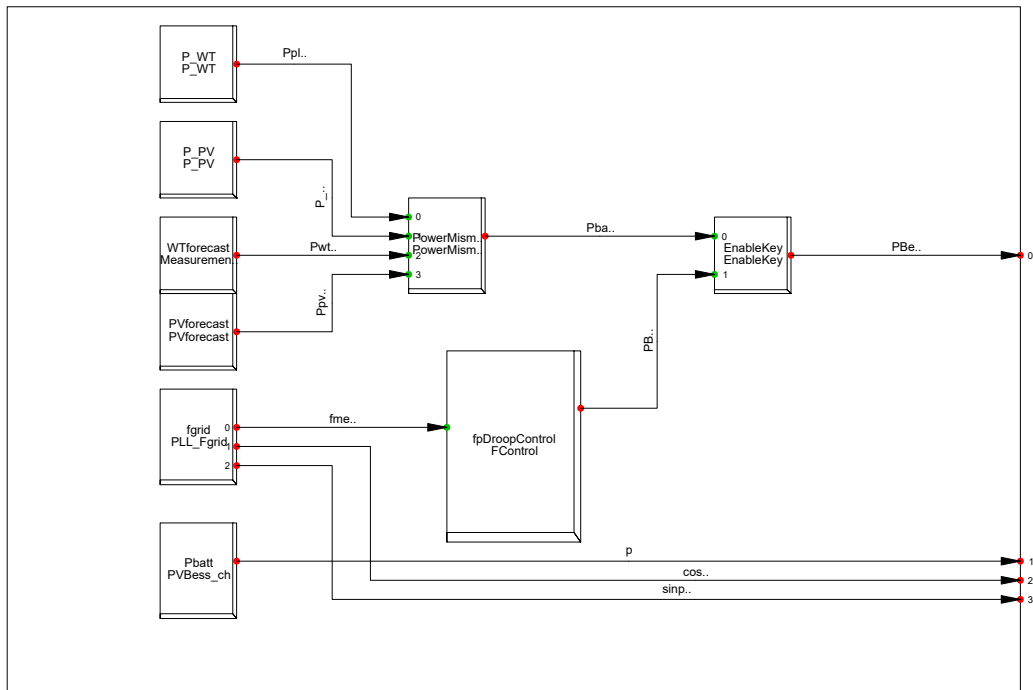


Figure C.1: Schematic representation of the HPP controller DSL model developed in PowerFactory.

C. PowerFactory Model Diagrams

F_Controller:

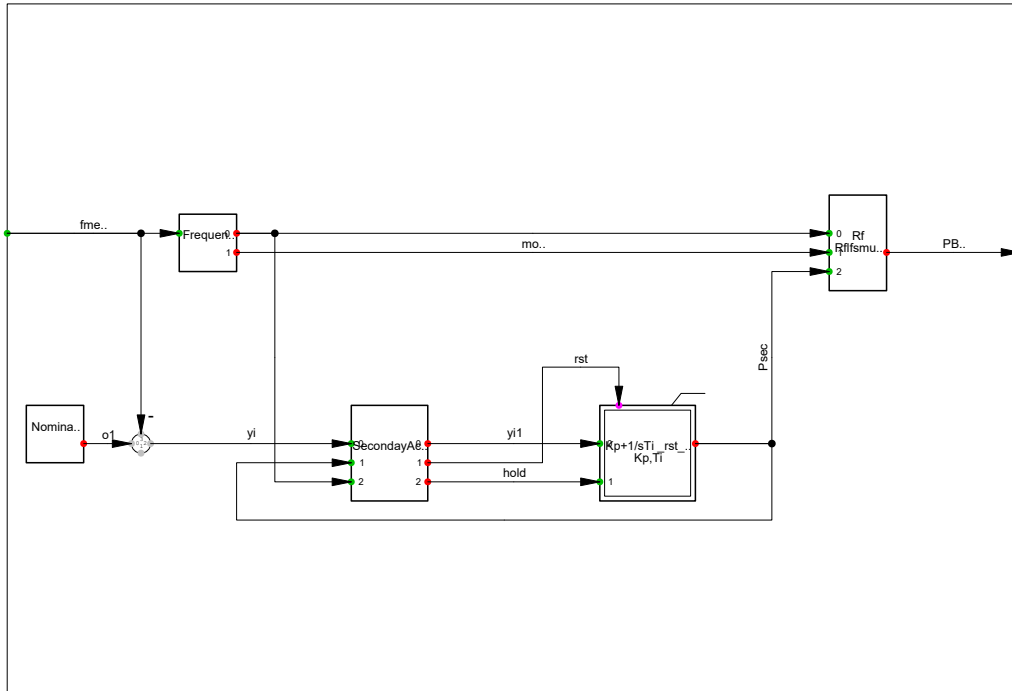


Figure C.2: Schematic representation of the frequency control included in HPP controller.

DispatchController:

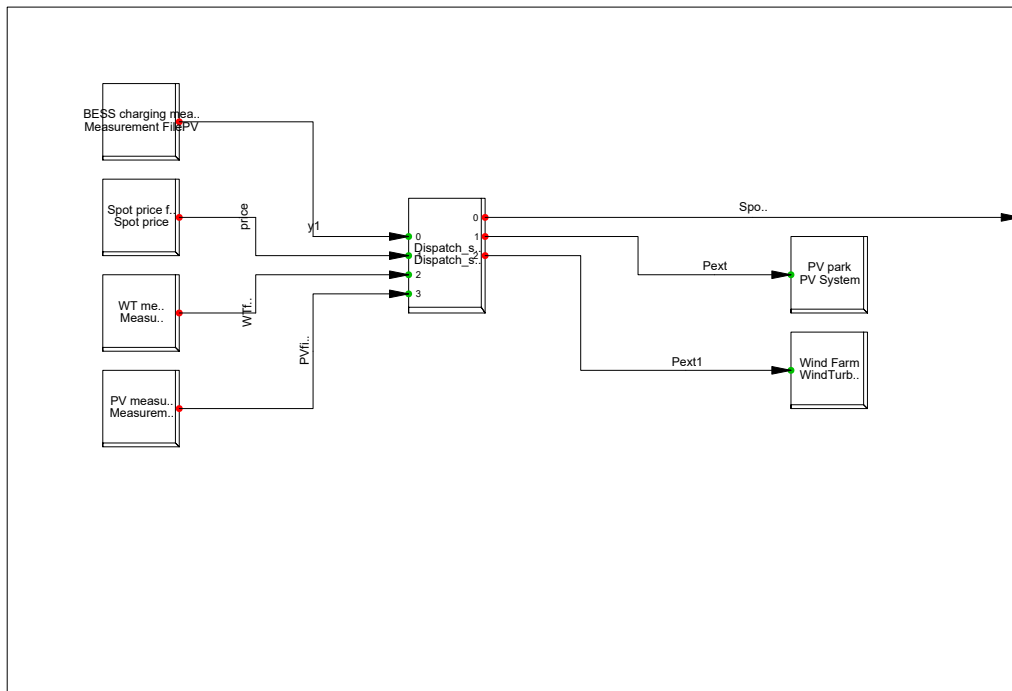


Figure C.3: Schematic representation of the dispatch controller DSL model.

C. PowerFactory Model Diagrams

BESS controller:

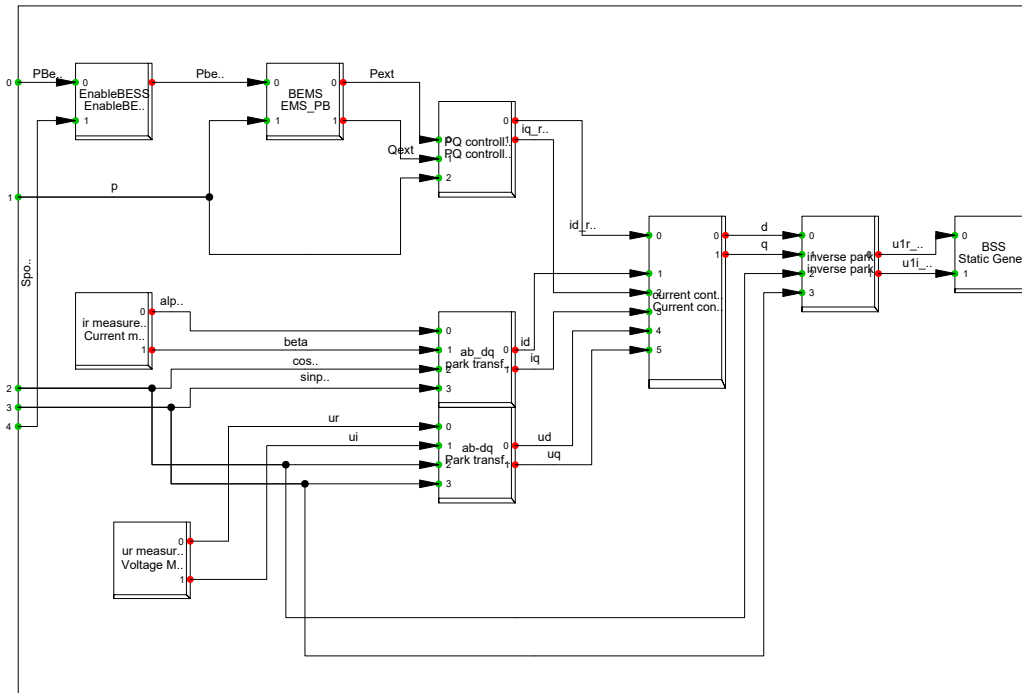


Figure C.4: Schematic representation of the BESS controller.

PQ controller:

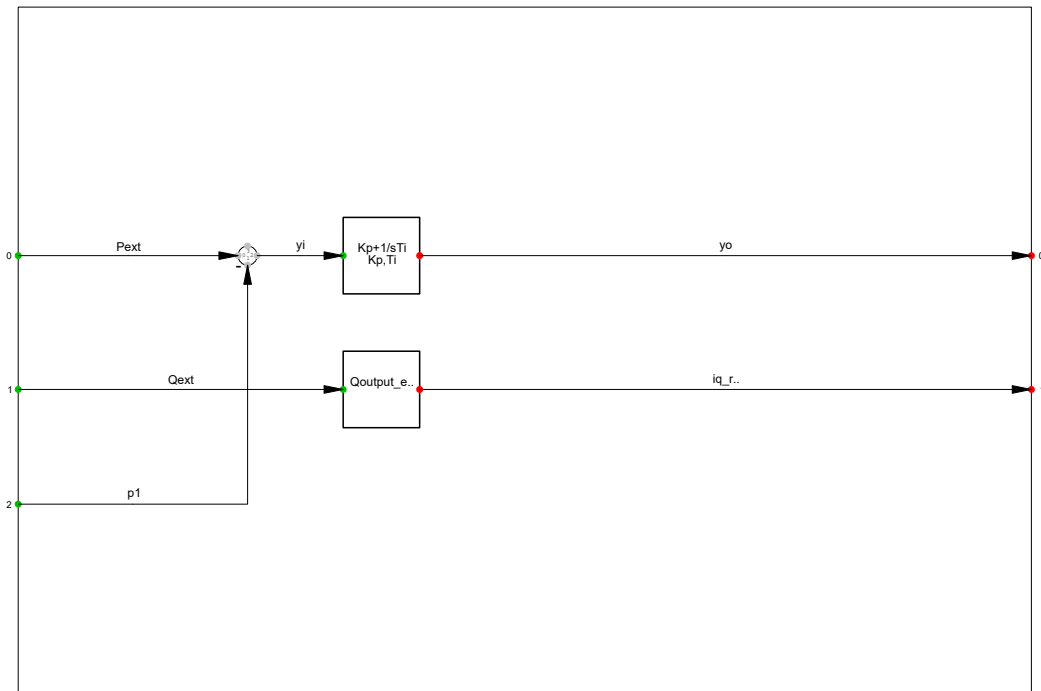


Figure C.5: Schematic representation of the P-Q control in the BESS controller.

Current Controller:

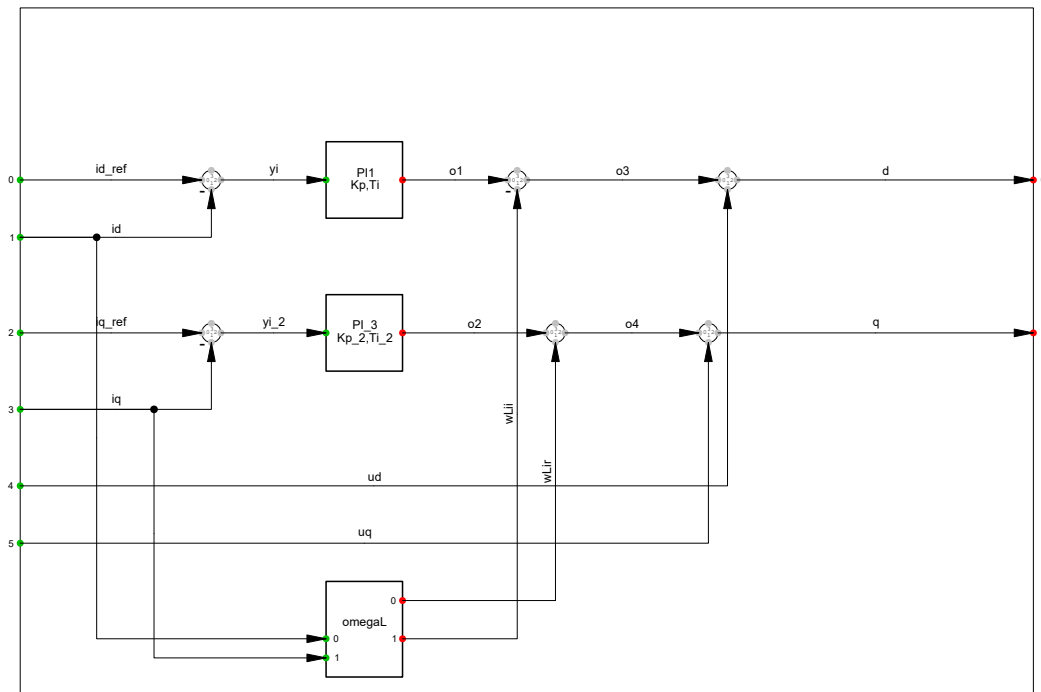


Figure C.6: Schematic representation of the current control in the BESS controller.

D Effect of Reset in PI controller

The effect of the *reset* parameter in the PI controller is depicted in Figure D.1. The top figure shows the generated reference for the secondary AS by the PI controller without the reset function. It is observed that the reference signal (shown in red) keeps on increasing linearly as the error never approaches zero due to insufficient power support. This if left unchecked will eventually lead to integrator windup. Introducing the reset parameter to make the error signal zero after the error reaches a particular value (e.g. 25MW), causes the reference power signal to behave as shown in the bottom figure.

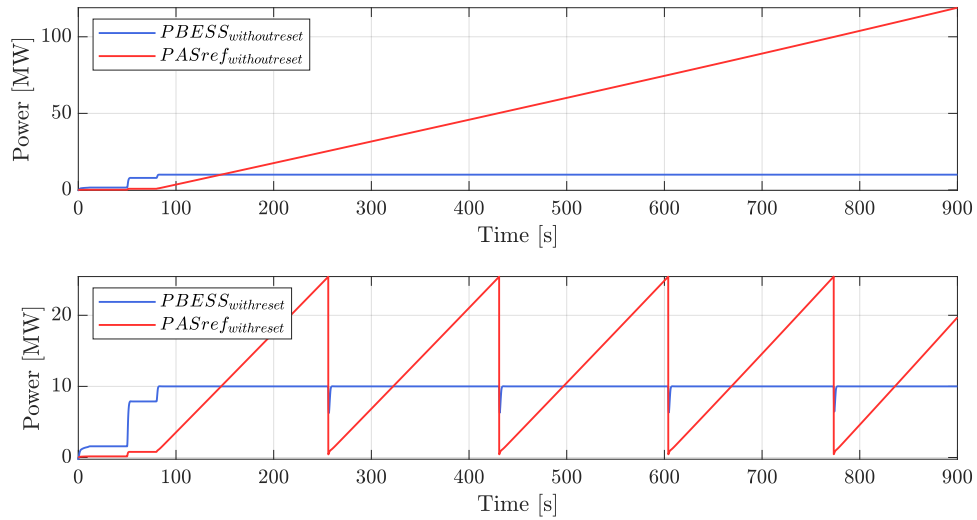


Figure D.1: Secondary response reference power signal for BESS with and without reset.

This modification improves the overall modelled system performance by limiting the error and thus, making the controller faster in case the signal changes from up-regulation to down-regulation or vice-versa as shown in Figure D.2.

D. Effect of Reset in PI controller

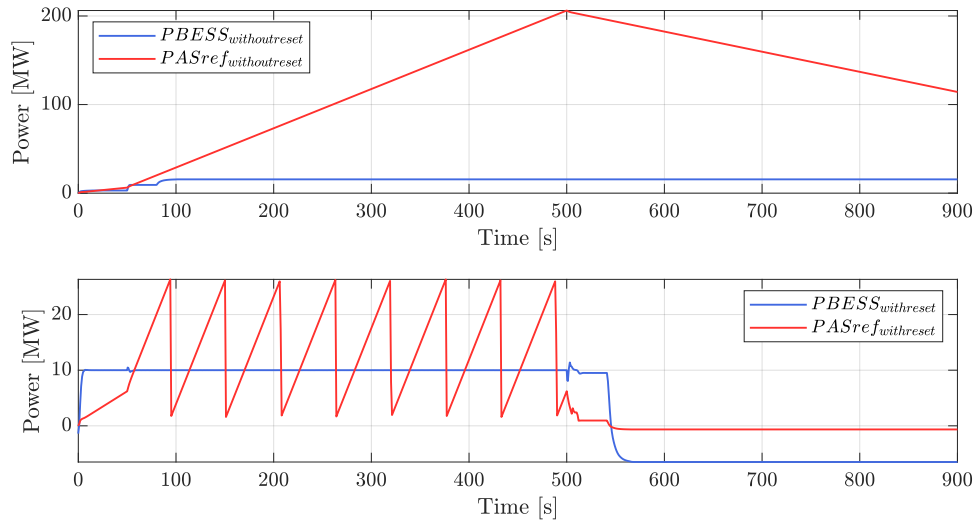


Figure D.2: Secondary response reference power signal for BESS with and without reset for upward and downward regulation.

E BMS DSL code

```
1  ! Initialisation of input and output parameters
2  inc(PBessRef)=0;
3  inc(Pext)=0;
4  inc(Qext)=0;
5  Qext=0; ! Reactive power refrence is set to zero
6  inc(p)=0; ! Measured power delivered by BESS
7  inc(Pbess)=0;
8
9  !! Definition of the System Parameters
10 !C_bat,SOC_ini
11 vardef(C_bat)='MWh';': BESS Capacity';
12 vardef(SOC_ini)='%';': Initial SOC of BESS';
13 vardef(Prated)='MW';': Converter rating of BESS';
14
15 inc(BESS_Cap)=C_bat*3600/Prated; ! BESS energy in p.u
16
17 !Initialisation of state variables
18 inc(SOCx)=SOC_ini; ! Initial state of charge
19 SOCx. =-p/BESS_Cap*100; ! Based on measured output power ...
    in p.u.
20
21 !! Initialisation of parameters
22 !SOC_T
23 !Calculation of SOC at any particular time
24 ! Limit state of charge at time t (20%-100%)
25 inc(SOC_T)=SOCx;
26 SOC_T = limstate(SOCx,20,100) ! BESS storage is limited ...
    to 20%-100% capacity,
27
28 !! Calculation of charging condition
29 !cc1,cc2,cc
30 inc(cc1)=0;
```

```

31 cc1= select(flipflop(SOC_T≥100,SOC_T≤90),0,1) ! 1 means ...
    ready to charge
32 inc(cc2)=0;
33 cc2= select(PBessRef>0,1,0) ! charge according to ...
    P_BessRef from HPPController
34 inc(cc)=0;
35 cc=select(cc1=1.and.cc2=1,1,0)
36
37 !! Calculation for discharging condition
38 ! dc1, dc2,dc
39 inc(dc1)=0;
40 dc1=select(flipflop(SOC_T≤20,SOC_T≥40),0 , 1) ! 1 means ...
    ready to discharge
41 inc(dc2)=0;
42 dc2= select(PBessRef<0,1,0); ! PbessRef>0
43 inc(dc)=0;
44 dc=select(dc1=1.and.dc2=1,1,0)
45
46 !! Charging power in p.u.
47 inc(Pbess_char)=0;
48 inc(Prefchar)=0;
49 Prefchar=min(1,abs(PBessRef)); !Limit can't exceed ...
    Prated i.e 1p.u
50 Pbess_char=-Prefchar*cc; ! Reference charging power of ...
    BESS in p.u..
51
52 !! Discharging power in p.u.
53 inc(Pbess_dis)=0;
54 inc(Prefdis)=0;
55 Prefdis=min(1,abs(PBessRef)); !Limit can't exceed Prated ...
    i.e 1p.u
56 Pbess_dis=Prefdis*dc; !Reference discharging power of ...
    BESS in p.u.
57
58 Pbess=Pbess_char+Pbess_dis
59 Pext=Pbess ! BESS reference in p.u.

```


F Case 1: Forecast Matching Results

Figure F.1 shows the power support capacities from the various sizing tests that are implemented when the BESS has a capacity of 5 MW and 10 MW with different initial SoC settings. The same process is followed for a BESS capacity of 20 MW illustrated in the second Figure F.2.

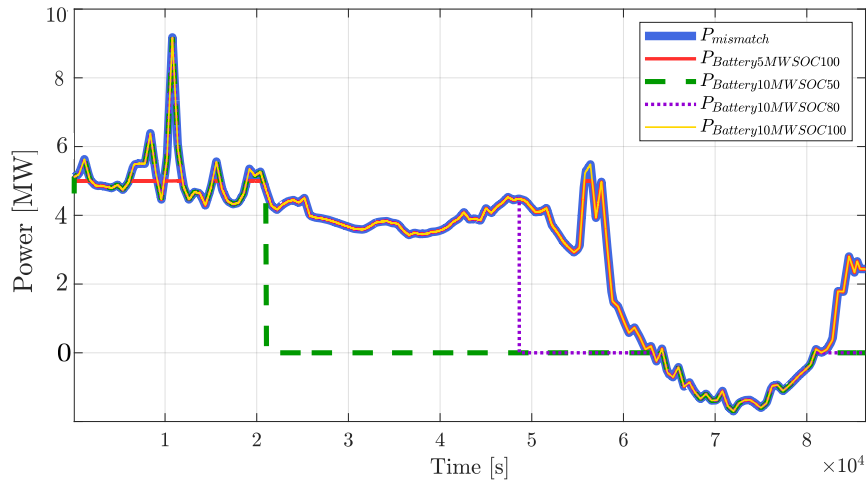


Figure F.1: Power mismatch signal and battery power for 5 MW and 10 MW.

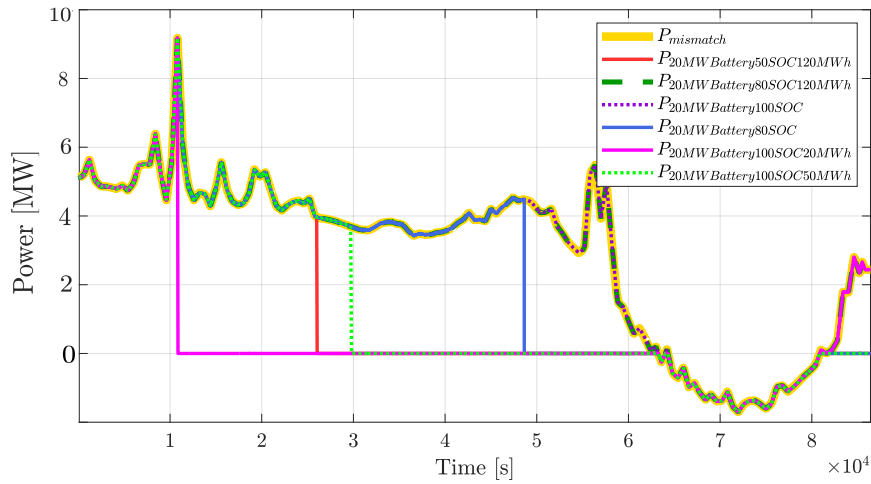


Figure F.2: Power mismatch signal and battery power for 20 MW.